ACS Partner Journal

ENVIRONMENT & HEALTH

Editors' Choice

Open Access

pubs.acs.org/EnvHealth

Article

Pollutant Exposure Shapes Mitochondrial Bioenergetics in a Wild Seabird

Guadalupe Lopez-Nava, Lucie Michel, Giacomo Dell'Omo, Petra Quillfeldt, Paco Bustamante, and Stefania Casagrande*

Cite This: *Environ. Health* 2026, 4, 782−799

Read Online

ACCESS | Metrics & More | Article Recommendations | Supporting Information

ABSTRACT: Laboratory studies show that mercury (Hg) and per- and polyfluoroalkyl substances (PFAS) can impair mitochondrial bioenergetics, which is a vital process for cellular energy production. However, their effects on wild, free-living organisms remain unexplored. Using red blood cells, we investigated how foraging habits, inferred from stable isotopes, and contaminant exposure were associated with mitochondrial bioenergetics in breeding Scopoli's shearwaters (*Calonectris diomedea*), a top marine predator in the Mediterranean Sea. We found higher concentrations of Hg, but not of total PFAS, in older individuals and in males compared to females. Our results also indicate dietary pollutant exposure: Hg, but not total PFAS, was higher in birds with a higher trophic position and in those foraging closer to shores. Additionally, higher Hg concentration was linked to higher mitochondrial proton leakage (LEAK), reflecting reduced efficiency to couple oxygen consumption to energy production. In contrast, specific PFAS were negatively associated with LEAK, suggesting a potential impairment in the regulation of mitochondrial membrane potential through proton conductance, a key mechanism protecting cells from oxidative stress. Our study highlights how foraging ecology shapes pollutant exposure and its consequences for mitochondria bioenergetics in an apex predator of conservation interest.

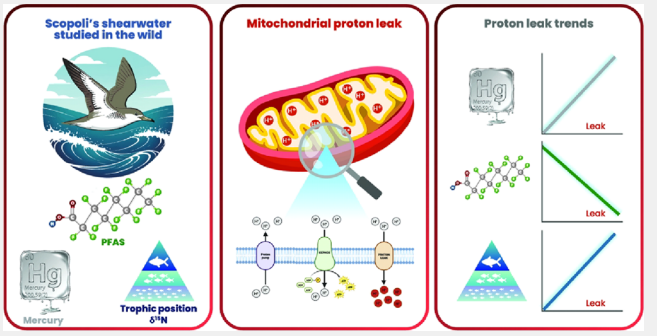

KEYWORDS: *mercury (Hg), mitochondrial bioenergetics, proton leakage (LEAK), oxidative phosphorylation (OXPHOS), PFAS (per- and polyfluoroalkyl substances), stable isotopes, diet, Scopoli's shearwater (Calonectris diomedea), marine ecotoxicology*

1. INTRODUCTION

Marine pollution is one of the most pressing human-induced threats impacting the world's oceans at different scales in the Anthropocene era.[1] This stressor is altering the chemistry and health of the oceans, disrupting food webs and threatening the survival of marine species and human well-being.[2] The oceans are the ultimate sink and accumulator for various chemical contaminants, including mercury (Hg)[3] and per- and polyfluoroalkyl substances (PFAS),[4] which have been detected globally in humans and wildlife, often at elevated concentrations.[5]

PFAS are synthetic chemicals known for their environmental persistence and resistance to degradation due to their surfactant properties, oil and water repellency, and high-temperature stability. They are typically released into the environment as either products or byproducts of various industries.[6] Hg, on the other hand, is a metal of global concern because of the health threats associated with the bioaccumulation in organisms and the biomagnification of its methylated form in aquatic food webs.[7] Even at low concentrations, Hg[8] and PFAS can be particularly toxic. These contaminants enter marine ecosystems primarily through atmospheric routes and surface runoff. The main sources of human-induced Hg pollution are industrial activities, coal combustion, waste disposal, mining, and cement production.[9] PFAS emissions originate from various anthropogenic sources, including wastewater treatment plants, as well as improper waste disposal and industrial discharges into rivers, which can ultimately carry PFAS to the oceans.[10] Once in the ocean, Hg, although less clear for PFAS, accumulates in sediments and biota and biomagnifies along the food webs.

Marine top predators are ideal candidates for monitoring chemical pollutants in the environment due to their high trophic position, long lifespan, and wide migratory ranges, which allow them to integrate and reflect temporal and spatial variations in contamination levels within their tissues.[11−13] However, the potential of chemical contaminants to impact key subcellular processes remains largely unexplored. Although previous studies

Received: July 14, 2025
Revised: December 9, 2025
Accepted: December 12, 2025
Published: December 22, 2025

https://doi.org/10.1021/envhealth.5c00297
Environ. Health 2026, 4, 782−799

have reported the impacts of both Hg and PFAS on their endocrine system,[14] reproductive health[15] and breeding success[16,17] to our knowledge, no studies on free-living organisms have investigated whether these contaminants have the potential to disrupt fundamental subcellular processes, such as those responsible for energy cell production.

The mitochondrial energetic metabolism encompasses several biochemical processes aimed at supplying most of the organismal energy currency, adenosine triphosphate (ATP), through the process of oxidative phosphorylation (OXPHOS). However, not all mitochondrial respiration is efficiently coupled to ATP production. Some energy is dissipated due to protons "leaking back" across the inner mitochondrial membrane without driving ATP synthesis, a process known as LEAK. Proton leakage across the inner mitochondrial membrane can occur either as a passive, constitutive process that controls the magnitude of the mitochondrial membrane potential or as an induced process that further decreases or increases mitochondrial efficiency.[18] Measuring mitochondrial metabolic traits, including this residual respiration, provides valuable insight into the efficiency of aerobic metabolism and potential imbalances in energy production.

Chemical pollutants such as Hg and PFAS pose potential risks to cellular and subcellular processes due to their chemical properties. Experimental evidence has shown that Hg can disrupt lipid cell membrane functions, leading to structural changes.[19] In the case of mitochondria, such disruptions might lead to alterations of the inner mitochondrial membrane, increasing membrane permeability and proton leakage. In vitro studies using red blood cells (RBCs) of humans have demonstrated that Hg induces alterations to specific membrane proteins like Ankyrin and Flotilin-2, which are essential for membrane cytoskeleton linkage.[19] Additionally, dietary exposure to Hg in laboratory rats reduced glutathione levels, which is a vital antioxidant and redox regulator, while also decreasing glutathione peroxidase and superoxide dismutase (SOD) activity. This depletion of antioxidant agents resulted in the exacerbation of oxidative damage to membrane lipids and proteins,[20] underscoring the effects of Hg exposure on cellular integrity. Indeed, in the PC12 rat cell line,[21] Hg exposure induced oxidative stress and led to a near-complete inhibition of mitochondrial respiration in neurons. On the other hand, proton leak can protect against oxidative stress by reducing the mitochondrial membrane potential, thereby limiting excessive production of reactive oxygen species (ROS) at the electron transport chain.[22] However, this condition can increase mitochondrial permeability, thereby fueling mitochondrial inefficiency to couple ATP.[22]

PFAS, due to their amphiphilic nature, particularly their lipophilic properties, are likely to adhere to the negatively charged mitochondrial matrix.[22,23] Mounting evidence indicates that PFAS elicits biphasic, concentration-dependent effects on mitochondrial bioenergetics. At sub-to-low-μM exposures, long-chain carboxylates such as perfluorodecanoic acid (PFDA) and perfluorooctanoate (PFOA) behave as classical mild uncouplers.[23] This increase in LEAK respiration lowers the ATP/oxygen ratio but dissipates the membrane potential, thereby limiting further electron leak and ROS formation, a response generally regarded as cytoprotective. In contrast, mid- to high exposures shift the response in the opposite direction. In isolated rat-liver mitochondria, PFDA produces a clearly biphasic response: concentrations rising to about 87.5 μg mL^{-1} drive a near-linear increase in LEAK oxygen consumption, consistent with partial uncoupling of the electron-transport system from oxidative phosphorylation. Once this threshold is exceeded, however, further additions (>87.5 μg mL^{-1}) progressively depress LEAK respiration.[24] Mechanistically, high membrane loading of PFAS is thought to stiffen the inner phospholipid bilayer or occlude proton-conductance pathways. A fall in LEAK at high PFAS burdens elevates the coupling efficiency. While this temporarily improves mitochondrial efficiency (e.g., zebrafish larvae exposed to high PFAS concentration increase development rate[25]), the steeper membrane potential increases the probability of single-electron slippage, thereby accelerating ROS formation. Lower uncoupling states are, therefore, potentially "energy-efficient but pro-oxidant," a scenario supported by the concomitant surge in ROS reported for highly exposed cells in independent bioenergetic studies. Recognizing this dose-dependent effect on LEAK is crucial to understanding the physiological challenges that PFAS pose to living organisms.

It is only recently that assessing such effects on wild populations has become accessible through minimally invasive methods. Highly sensitive technologies measuring cellular energetics now provide a unique opportunity to assess respiratory activity at the cellular level of tissues that show low oxygen consumption, like blood. Blood metabolism has been shown to be a reliable proxy for organismal metabolism in birds[26,27] and mammals,[28] including humans.[29] These advancements thus offer a valuable tool to assess the impacts of contaminants at a subcellular level in free-living and wild populations, which are at the highest risk of the physiological effects of pollutant exposure.

Despite the implementation of stricter regulations in recent years,[30] Hg and PFAS still persist in the oceans and continue to pose significant threats to the ecosystems.[31,32] Consequently, understanding their impact on mitochondrial bioenergetics in wild populations is crucial for evaluating broader ecological risks. The Scopoli's shearwater (*Calonectris diomedea*) serves as an ideal model to assess the potential impacts of chemical pollutants on key mitochondrial bioenergetic traits. The consistent detection of Hg[33,34] and PFAS[12,13] in their tissues highlights their exposure to these contaminants. As marine apex predators with high trophic levels, shearwaters are particularly vulnerable to physiological risks associated with contaminant exposure,[35] likely due to their diet and foraging patterns. Diet composition is essential not only for meeting the energetic demands of fitness-related activities, such as breeding and migration, but also for providing the primary substrates necessary for subcellular energy production, thereby influencing energy-related processes. Scopoli's shearwaters primarily feed on epipelagic small- to medium-sized fish, crustaceans, and cephalopods.[36] However, since they are opportunistic feeders, their diet can vary among localities and years, influenced by prey availability and abundance, oceanographic conditions, and the locations of foraging areas.[37] Additionally, other food sources include trawl discards and bait used in longline fishing, further contributing to the variability in their dietary intake.[38] Due to the complexity of the interplay between foraging patterns, contaminant exposure, and their potential combined effects on mitochondrial function, it is convenient to assess their respective contributions. To this extent, the use of stable isotopes (SIs), such as δ^{15}N and δ^{13}C, detected in the blood can provide valuable insights into understanding exposure to environmental pollutants through diet composition and foraging patterns. Specifically, δ^{15}N reflects nitrogen enrichment that occurs with each step up the food chain (i.e., from primary producers to

https://doi.org/10.1021/envhealth.5c00297
Environ. Health 2026, 4, 782−799

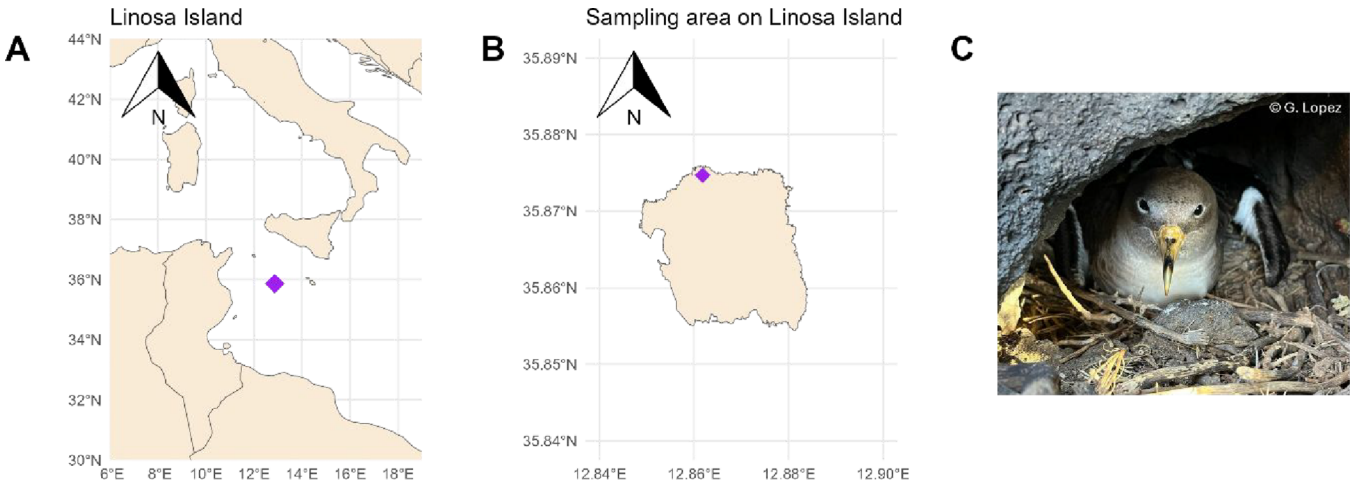

Figure 1. Study area of Scopoli's shearwaters. (a) Location of Linosa Island (in purple) in the Sicilian channel; (b) sampling area (in purple) located in the northern part of the island ("Mannarazza"); (c) adult Scopoli's shearwater inside its breeding nest.

fourth-grade consumers), making it a reliable proxy for an organism's trophic position.[39] On the other hand, $\delta^{13}C$ is used to differentiate between carbon sources, such as those from oceanic versus littoral zones, serving as a proxy for habitat use and resource partitioning.[39] Moreover, unlike mammals, birds retain nucleated RBCs containing functional mitochondria, which allow for direct measurement of subcellular respiration rates,[18,40] providing a minimally invasive window into bioenergetic function in wild animals.

Using SIs, contaminant analyses, and assessments in RBCs of mitochondrial bioenergetic function, we aimed to understand how contaminant exposure influences mitochondrial bioenergetic traits in breeding shearwaters. We hypothesized that contaminant levels during the chick-rearing period would vary based on (1) individual features, with higher concentrations of both Hg and PFAS expected in (i) older individuals due to time-dependent bioaccumulation and (ii) in males compared to females because of the clearance of contaminants during the production of the large egg, laid by females typically almost every year. (2) SIs, as proxies for contaminant exposure patterns, predicting higher values of both Hg and PFAS (i) in individuals with a higher trophic position (higher $\delta^{15}N$), due to biomagnification of contaminants in predators higher in the food web; (ii) in individuals foraging closer to the shore (higher values of $\delta^{13}C$), from where pollutants reach the sea. (3) We also hypothesized that contaminant concentrations would be associated with alterations in mitochondrial bioenergetic traits, but with different patterns depending on the contaminant. Specifically, we expected higher mercury concentrations to be associated with increased LEAK respiration, reflecting mitochondrial inefficiency in coupling of respiration with ATP production. Given the biphasic nature of PFAS effects (mean exposures acting as uncouplers that increase LEAK, and high exposures hyperpolarizing the membrane and tightening coupling), we predicted that LEAK respiration would decrease at the concentrations of PFAS expected for this population; (4) SIs indicating higher exposure to Hg and PFAS will affect mitochondrial bioenergetic functions.

2. MATERIALS AND METHODS

2.1. Field Study Design

Fieldwork was conducted during the reproductive seasons of 2020 and 2021 (chick rearing phase) in a Scopoli's shearwater colony on Linosa island (5.43 km^2), located in the Sicilian channel at 35°51′33″N; 12°51′34″E (Figure 1a), with sampling periods ranging from August 7 to 19, 2020, and July 28 to August 6, 2021. The colony is primarily concentrated in the northern region of the island, known as "Mannarazza" (Figure 1b). We investigated a total of 52 adults (n = 21 in 2020 and n = 31 in 2021), capturing them in their nests at night between 22:20 and 00:45. To minimize disturbance and avoid interfering with food provisioning to chicks, we conducted captures approximately 1−2 h after the adults' return to the colony, rather than immediately upon their arrival (Figure 1c). During this breeding phase, shearwaters return to the colony after sunset to feed their single-sired chick inside nests situated within natural caves and crevices on the island's volcanic landscape. Individuals previously identified through validated molecular sexing techniques,[41] were recognized by their unique ring numbers attached to their tarsus. The age of all identified individuals is known in years. Birds ringed as fledglings have their ages recorded accurately, while those ringed as adults are assumed to be at least 6 years old, the typical age of reproductive maturity.[42] Prior to this age, individuals are rarely observed establishing a breeding nest with a partner in the colony. Shearwaters show high nest fidelity, and if they change nests, they do it in close proximity to their previous nest (usually less than 8 m and rarely more than 100 m).[43] As a result, any change in a breeding individual in a given nest is easily detected across and within the breeding season, making it unlikely that a newly ringed adult is significantly older than assumed.

2.2. Blood Collection

We captured breeders inside or very close (0.5−1 m distance) to their recorded nest sites. After capture, we collected a blood sample of a maximum of 400 μL from the tarsal vein using a heparinized syringe and a 25-gauge needle. We only considered blood samples taken within 5 min of capture to ensure the determination of baseline physiological parameters before metabolic stress is induced by handling.[40] The blood samples were immediately transferred into heparinized tubes and kept on ice inside a small laboratory cooler containing two artificial ice blocks, one at the bottom and one on top of the samples. Based on our experience, this setup effectively maintains samples at a low and stable temperature throughout the fieldwork period, particularly during nighttime sampling when all collections were conducted. Upon return to the lab, the samples were centrifuged at 2000 g (relative centrifugal force, i.e., times the force of gravity) for 10 min to separate plasma and RBCs. Mitochondrial bioenergetic analysis was performed within 5 h of collection and in RBCs, as they are metabolically active in birds.[18,40] The remaining RBCs were used to quantify Hg and PFAS concentrations as well as SIs values.

2.3. Mitochondria Bioenergetic Traits

Oxygen consumption in the RBC during mitochondrial respiration was measured using a high-resolution respirometry chamber (Oxygraph-2k,

https://doi.org/10.1021/envhealth.5c00297
Environ. Health 2026, 4, 782−799

Orobos Instruments, Innsbruck, Austria). The RBCs were transferred into 1 mL of cold Mir05 buffer for washing, which contained 0.5 mmol L^{-1} EGTA, 3 mmol L^{-1} $MgCl_2$, 60 mmol L^{-1} potassium lactobionate, 20 mmol L^{-1} taurine, 10 mmol L^{-1} KH_2PO_4, 20 mmol L^{-1} Hepes, 110 mmol L^{-1} sucrose, 15 mmol L^{-1} fatty acid-free bovine serum albumin, at pH 7.1. To minimize contamination with other blood cells, the RBC sample was collected from the bottom of the tube. The cells were centrifuged at 500 *g* for 5 min, and the supernatant was discarded. The pellet was then resuspended in 1 mL of Mir05 buffer pre-equilibrated at 40 °C (average body temperature recorded for the population; unpublished own data) in a Clark-type electrode high-resolution respirometer chamber (Oxygraph-2k, Orobos Instruments, Innsbruck, Austria). Mitochondria respiration was quantified as oxygen (O_2) consumed by intact cells at the following stages: (1) cellular metabolic rate (CMR): basal respiration (often referred to as "ROUTINE") of the cells in their natural state; (2) Proton leak (LEAK): measured by inhibiting ATP synthase through the addition of 1 μg mL^{-1} oligomycin. This parameter represents residual respiration not coupled to ATP synthesis, releasing heat (also referred to as "uncoupled respiration" or "nonphosphorylation respiration"); (3) OXPHOS: the remaining basal respiration not affected by oligomycin and provides the quantification of oxidative phosphorylation through which ATP is produced; (4) electron transport system (ETS) capacity: assessed by adding the mitochondrial uncoupler carbonyl cyanide *m*-chlorophenyl hydrazone (CCCP) through titration with 1 μg mL^{-1} aliquots. Basal respiration is limited to ATP production demands, whereas mitochondrial uncoupler allows electron flow through the ETS to occur independently of ADP to ATP conversion. This uncoupled condition serves as a reliable indicator of the state of the ETS and its capacity to transport and oxidize energy substrates.[18,40] All respiration traits were corrected for nonmitochondrial O_2 consumption by adding antimycin (5 μmol^{-1}), a potent mitochondria suppressor. From these measurements, mitochondrial inefficiency (FCR_1, coupling efficiency index) was calculated, reflecting the coupling of respiration with ATP production relative to the maximal respiration capacity. This is expressed as the proportion of LEAK to CMR respiration: (LEAK/CMR). All measurements were normalized to the volume of RBCs used in the analysis (30 μL) and expressed as pmol of the O_2 sec^{-1} mL^{-1} of RBCs.

2.4. Hg and Stable Isotope Analyses

The analyses of Hg and stable isotopes were conducted at the LIENSs laboratory (France). Hg concentrations and stable isotope values of carbon and nitrogen were measured in freeze-dried RBCs sampled in 2020 (females n = 12, males n = 9) and 2021 (females n = 17, males n = 14).

For the measurement of stable isotope values of carbon and nitrogen, we weighed in ∼0.3 mg aliquots of dried RBC in tin capsules. The folded tin capsules were then analyzed using a Delta V Plus isotope ratio mass spectrometer equipped with a Conflo IV interface (Thermo Scientific, Bremen, Germany) and a Flash 2000 elemental analyzer (Thermo Scientific, Milan, Italy). Certified reference materials were used for calibration with a two-point calibration method employing the working standards USGS-61 (caffeine) and USGS-63 (caffeine). Internal laboratory standards, acetanilide (Thermo Scientific) and peptone (Sigma-Aldrich), were analyzed together with the samples, achieving an analytical precision of <0.15‰ for δ^{15}N and <0.10‰ for δ^{13}C. Results are presented in δ units, representing deviations from standards (Vienna Pee Dee Belemnite for δ^{13}C and atmospheric N2 for δ^{15}N), using the formula:

$$\delta 13C \text{ or } \delta 15N = [(R_{sample}/R_{standard}) - 1] \times 10^3$$

where R is 15N/14N or 13C/12C, respectively.

A sample amount of 0.2−0.8 mg (mean 0.4 mg) of freeze-dried RBCs was analyzed using an Advanced Mercury Analyzer spectrophotometer (Altec AMA 254). Each sample was measured 2−3 times until having a relative SD < 10%. Measurement quality was assessed by the certified reference material Tort-3 Lobster Hepatopancreas (NRC, Canada), whose certified Hg concentration was 0.292 ± 0.022, and our measured values were 0.301 ± 0.003 (n = 24). Blanks were analyzed regularly at the beginning of each working unit, and the limit of detection (LoD) was 0.005 μg g^{-1} dw. Results are given in μg g^{-1} dw as means ± SD.

2.5. PFAS Analysis

PFAS concentrations were determined from RBCs of 20 adult shearwaters (females n = 12, males n = 9) in 2020 only. The PFAS analyses were carried out at the NTNU Trondheim, Norway. Standards for the targeted analysis of PFAS comprised 39 congeners, including 14 perfluoroalkyl carboxylates (PFCAs), 9 perfluorosulfonates (PFSAs), 4 fluorotelomere sulfonates (FTSs), 7 fluorosulfonamides, and 5 miscellaneous substitute compounds. A complete list of targeted PFAS congeners, internal standards, quantification details, and detection limits is presented in Michel et al.[13] Sample extraction followed the protocol presented by Michel et al., briefly between 30 and 130 mg of lyophilized RBCs were restored with 300 μL of water, spiked with 10 μL of 1 mg L^{-1} ^{13}C-isotope-labeled IS-mixture, and 600 μL of methanol containing 1% ammonium formate (w/v) was added. Extraction included vortexing (30 s), ultrasonication (30 min), and centrifugation (5 min, 3500 r/min), subsequently passing the supernatant through Hybrid-SPE cartridges and collection and storage of the extract for analysis in amber vials. Target analytes were determined using an Acquity UPLC I-Class system (Waters, Milford, CT, USA) coupled to a triple quadrupole mass analyzer (QqQ; Xevo TQ-S) with a ZSpray ESI ion source (Waters, Milford, CT, USA). Chromatic separation was performed with a Kinetex C18 (30 × 2.1 mm, 1.3 μm) connected to a Phenomenex C18 guard column (2.0 × 2.1 mm). The instrument method used has first been described by Sait et al.,[44] and the measures taken to ensure quality assurance and quality control are described in Michel et al.[13]

UPLC−MS/MS data from the PFAS analysis were acquired with MassLynx v4.1 software, and quantification was performed with TargetLynx (Waters, Milford, CT, USA). Excel (Microsoft, 2018) was used to calculate the PFAS concentrations of peak areas detected for the target analytes in the samples, and are reported in ng g^{-1} dry weight. Values below the detection limits were reported using the corresponding lowest value (see Table S1 for the detection limits of each chemical).

2.6. Statistical Analysis

We analyzed variation in contaminant levels using an LMM for Hg and a GLMM (Gamma, log link) for ΣPFAS, with sex, age, and body mass as fixed effects, nest identity as a random intercept and year included only for Hg (ΣPFAS available only for 2020). We then assessed the relationship between stable isotopes (δ^{15}N, δ^{13}C) and contaminants using an LMM for Hg and a GLM (Gamma, log link) for ΣPFAS, prioritizing statistical power given the single-year PFAS data set. To test how contaminants and stable isotopes influence mitochondrial bioenergetic traits (CMR, OXPHOS, ETS, LEAK, FCR1), we fitted LMMs including sex, age, body mass, and year (except PFAS models) with nest identity and mitochondrial analysis time as random intercepts; age and body mass were standardized (1 SD). Because specific PFAS compounds detected during chick rearing may affect mitochondrial function (19), we conducted a Web of Science search ("PFAS name" AND "mitochondri*") and fitted GLMs (Gamma, log link) testing each compound against mitochondrial traits. Fixed effects that did not explain meaningful variation in ΣPFAS in previous models were excluded to optimize the statistical power. Model assumptions were checked using residual diagnostics,[45] overdispersion tests, and VIFs (<2). For LMMs, we used the BOBYQA optimizer with increased iterations, and extracted posterior simulations (10,000 draws) with the "sim" function.[46] We report marginal/conditional R^2, σ^2, τ00, and ICC.[47] All analyses were performed in R 4.3.2[48] using lme4[49] and plots generated with ggplot2.[50]

Full methodological details and justification of model structures are provided in the Supplementary Methods.

3. RESULTS

We present observed concentrations of Hg and Σ PFAS, as well as values of SIs (δ^{15}N and δ^{13}C), in blood samples of Scopoli's shearwaters, stratified by sex and summarized using descriptive

https://doi.org/10.1021/envhealth.5c00297
Environ. Health 2026, 4, 782−799

Table 1. Estimates Derived from (a) a LMM for Mercury (Hg) Concentrations (ng mg^{-1}) and from (a, b) GLMM (Gamma Distribution) for Σ PFAS Levels (ng g^{-1})

	(a) Hg	(b) Σ PFAS
(marginal R^2/conditional R^2)	(0.360/0.430)	(0.105/0.525)
fixed effects		
	β (95% CrI)[a] p[b]	β (95% CrI)[a] p[b]
intercept	3.49 (2.70, 4.27) ***	4.34 (3.54, 5.13) ***
year: year2021	0.96 (−0.16, 1.97)	NA
sex: male	**1.91 (0.77, 3.07) ** **	0.35 (−1.35, 2.04)
age[c]	**0.56 (0.11, 1.01) ***	0.23 (−0.73, 1.19)
body mass[c]	−0.18 (−0.80, 0.4)	−0.15 (−1.03, 0.70)
random intercepts		
σ2	2.36	0.13
τ00 nest	0.00	0.11
ICC	0.00	0.47
N nest	31	15
observations	52	21

[a]Slope β is given for fixed effects. Confidence intervals (CI) and credible intervals (CrI) not overlapping zero are marked in bold. [b]Significance of fixed effects in the frequentist LMM and GLMM is given as ***p < 0.001, **p < 0.01, and *p < 0.05. Note that we did not calculate p-values for effects whose CrI overlapped zero. [c]Scaled/centered around the mean.

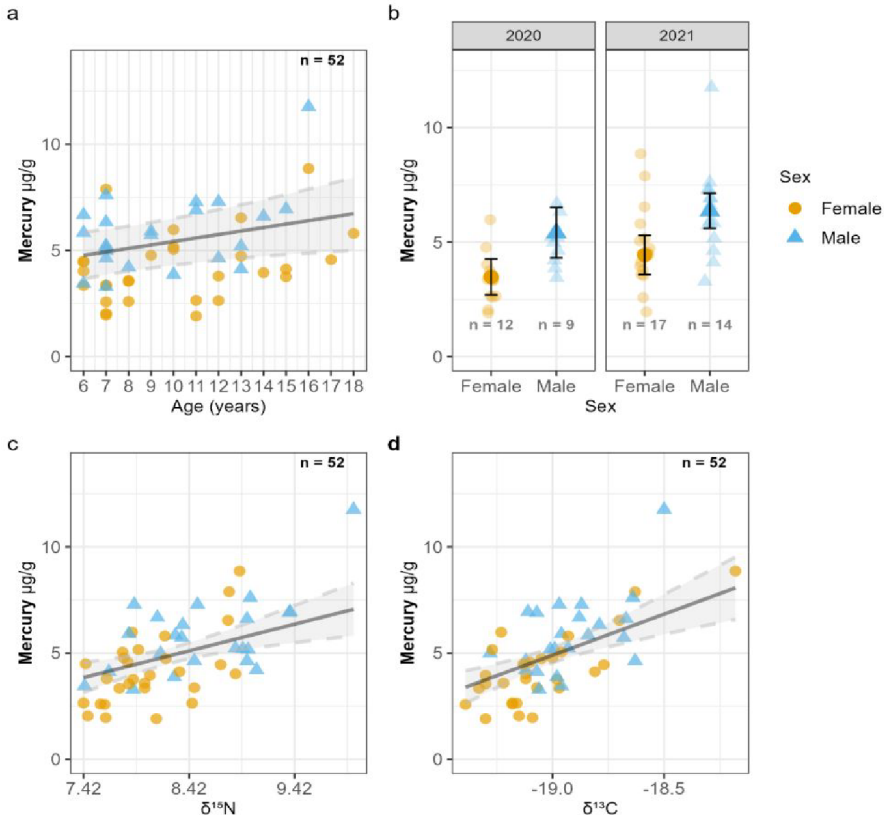

Figure 2. Mercury variation among individual traits in Scopoli's shearwaters. Linear mixed-effects models showed that (a, b) older and male individuals had higher Hg concentrations, and that (c, d) Hg concentrations increased with SIs values. Raw data are shown as semitransparent points. In (a, c, d), regression lines are shown as a thick line with shaded 95% CrI areas. In (b), predicted means are plotted as solid shapes and 95% CrI is indicated by error bars. Female data points are presented in yellow and male in blue.

statistics (sample size, mean ± SD, median, minimum, and maximum values) (Supporting Information, Table S1). Additionally, we present how mitochondrial bioenergetic traits varied with sex, age, and body mass based on models that exclude pollutants (Hg, Σ PFAS) and SIs (δ^{15}N and δ^{13}C) (Supporting Information, Figure S1).

3.1. Variation of Hg and PFAS Concentrations in Relation to Age, Sex, and Body Mass

As expected, older individuals showed higher Hg concentrations, as indicated by a positive association between Hg concentrations and age (Table 1a and Figure 2a). Males also showed higher Hg concentrations than females (Table 1a and Figure 2b). In contrast, we found no meaningful associations between Hg concentrations and either the year of sampling or

https://doi.org/10.1021/envhealth.5c00297
Environ. Health 2026, 4, 782−799

Table 2. Effect of δ^{15}N and δ^{13}C on (a) Mercury (Hg) (ng/mg) and (b) Σ PFAS (ng/g) Concentrations Measured in Blood Samples of Adult Scopoli's Shearwater during Chick-Rearing[a]

	(a) Hg	(b) Σ PFAS
(marginal R^2/conditional R^2)	(0.578/0.630)	(0.03/NA)
fixed effects		
	β (95% CrI)[b] p[c]	β (95% CrI)[b] p[c]
intercept	**4.91 (4.55, 5.28) *** **	4.55 (4.29, 4.80) ***
δ^{15}N[d]	**0.74 (0.33, 1.16) ** **	0.07 (−0.20, 0.34)
δ^{13}C[d]	0.92 (0.49, 1.32) ***	0.07 (−0.30, 0.45)
random intercepts		
σ2	1.35	NA
τ00 nest	0.19	NA
ICC	0.12	NA
N nest	31	NA
observations	52	21

[a]For Hg, estimates were derived from an LMM, while for Σ PFAS, they were derived from a GLM (gamma distribution). [b]Slope β is given for fixed effects. Confidence intervals (CI) and credible intervals (CrI) not overlapping zero are marked in bold. [c]Significance of fixed effects in the frequentist LMM is given as ***$p < 0.001$, **$p < 0.01$, and *$p < 0.05$. Note that we did not calculate p-values for effects whose CrI overlapped zero. [d]Scaled/centered around the mean.

the body mass (Table 1a). Similarly, Σ PFAS concentrations trended higher with age, and males appeared to show higher concentrations than females. However, these patterns were not statistically meaningful (Table 1b).

3.2. Associations between Hg and PFAS Concentrations and SIs (δ^{15}N and δ^{13}C)

Hg concentrations were associated with increases in δ^{15}N (Table 2a and Figure 2c) and δ^{13}C (Table 2b and Figure 2d). In contrast, we found no meaningful association between Σ PFAS and either δ^{15}N or δ^{13}C (Table 2b).

3.3. Associations between Hg, PFAS Concentrations, and Mitochondrial Bioenergetic Traits

Hg concentrations were positively associated with LEAK (Table 3d and Figure 3a), while no meaningful associations were observed between Hg concentrations and CMR, OXPHOS, ETS, or FCR_l (Table 3a−c,e, respectively). We observed no evidence of meaningful associations between Σ PFAS and any mitochondrial bioenergetic traits (Table 4). However, when assessing the influence of specific PFAS, we observed that perfluorohexane sulfonic acid (PFHxS), perfluoroheptane sulfonic acid (PFHPS), perfluorooctanesulfonic acid (PFOS), perfluorodecane sulfonic acid (PFDS), perfluorooctanoic acid (PFOA), perfluorononanoic acid (PFNA), perfluorodecanoic acid (PFDA), and perfluorododecanoic acid (PFDODA) were negatively associated with LEAK (Table 5 and Figure 3bi). Notably, PFOA and PFHPS were negatively associated not only with LEAK but also with FCR_l (Table 5 and Figure 4). PFDA was negatively associated with LEAK and CMR (Table 5 and Figure 5), and PFDS was negatively associated not only with LEAK but also with FCR_l, CMR, and ETS (Table 5 and Figure 5).

3.4. Relationships between SIs Related to Hg Exposure and Mitochondrial Bioenergetic Traits

δ^{15}N was associated with higher LEAK (Table 6d and Figure 6a) and FCR_l levels (i.e., mitochondrial inefficiency) (Table 6e and Figure 6b), indicating that the mitochondria of individuals with a higher trophic position were less coupled to ATP production. Interannual differences among mitochondrial bioenergetic traits were also evident, with CMR (Tables 3a and 6a), OXPHOS (Tables 3b and 6b), ETS (Tables 3c and 6c), and LEAK (Tables 3d and 6d) levels being higher in 2020 compared to 2021.

The limited variation in δ^{13}C, likely reflecting the restricted pelagic foraging range and dietary origin of chick-rearing shearwaters on Linosa,[13] and its evident correlation with δ^{15}N (Supporting Information: Figure S2) indicate redundant dietary information. Therefore, δ^{13}C was not further analyzed in relation to mitochondrial bioenergetics.

4. DISCUSSION

The primary aim of this study was to investigate how Hg and PFAS levels influence mitochondrial bioenergetic traits measured from blood samples in a wild sea bird population. Additionally, we explored potential drivers of pollutant exposure by using ecological proxies, such as stable isotopes, for trophic position and foraging habitat use, as these factors can influence exposure to Hg[17] and PFAS.[13] Our predictions were supported for Hg and specific PFAS compounds but not for summed exposure to PFAS. Only specific individual PFAS (i.e., PFOS, PFH_XS, PFNA, PFD_ODA, PFOA, PFH_PS, PFDA) meaningfully explained variation in mitochondrial bioenergetic traits, particularly LEAK respiration: birds carrying the highest concentrations of these congeners exhibited markedly lower LEAK respiration, consistent with the lower uncoupling expected at elevated exposure levels. Hg concentrations increased with higher δ^{15}N and δ^{13}C values (Figure 1c,d) and were positively associated with LEAK respiration (Figure 2), suggesting a potential link between Hg exposure and mitochondrial inefficiency in producing ATP. To the best of our knowledge, this is the first study to explore the potential associations between cellular bioenergetic traits, contaminant exposure, and stable isotope signatures in wild animals. Below, we discuss the implications of these findings in detail.

Shearwaters showed a relatively high exposition to Hg, with a mean (±sd) concentration of 4.91 ± 1.90 $\mu g\ g^{-1}$ (range: 1.91−11.76 $\mu g\ g^{-1}$). Notably, these values match or even exceed those reported in feathers and livers of other Mediterranean seabirds,[34] even though those tissues typically accumulate more Hg than blood.[51] By comparison, black-vented shearwaters (*Puffinus opisthomelas*) from the Pacific Mexican coast exhibited lower blood concentrations of 1.84 ± 1.90 $\mu g\ g^{-1}$ (range: 1.41−2.40 $\mu g\ g^{-1}$).[52] Further, the Hg concentrations observed here are within the range reported for seabird species at higher trophic positions, such as albatrosses, which have been

https://doi.org/10.1021/envhealth.5c00297
Environ. Health 2026, 4, 782−799

Table 3. Comparison of Linear Mixed-Effects Models: Estimates of the Effect of Hg Concentrations ($\mu g\ g^{-1}$) on Mitochondrial Bioenergetic Traits in Blood Samples of Adult Scopoli's Shearwaters

	(a) **CMR**	(b) **OXPHOS**	(c) **ETS**	(d) **LEAK**	(e) **FCR_l**
(marginal R^2/conditional R^2)	(0.393/0.726)	(0.273/0.576)	(0.282/0.804)	(0.437/0.682)	(0.177/0.514)
fixed effects					
	β (95% CrI)[a] p[b]	β (95% CrI)[a] p[b]	β (95% CrI)[a] p[b]	β (95% CrI)[a] p[b]	β (95% CrI)[a] p[b]
intercept	**381.84 (340.76, 423.97)** ***	233.69 (189.32, 275.16) ***	**538.53 (447.64, 631.80)** ***	**156.29 (131.93, 181.29)** ***	0.41 (0.33, 0.50) ***
Hg[c]	15.21 (−5.57, 37.06)	14.37 (−8.62, 38.52)	36.99 (−4.78, 80.90)	**18.35 (5.25, 32.11)** **	0.04 (−0.01, 0.08)
sex: male	−0.36 (−45.37, 45.40)	−4.92 (−55.38, 46.40)	−5.79 (−92.69, 82.61)	−12.84 (−41.54, 16.32)	−0.02 (−0.12, 0.08)
age[c]	−12.41(−33.93, 9.22)	−17.91 (−40.55, 4.97)	−15.90 (−65.06, 33.72)	−5.80 (−18.79, 7.32)	0.01 (−0.03, 0.06)
body mass[c]	−22.62 (−46.52, 1.49)	−12.76 (−38.92, 13.74)	−14.54 (−64.08 to 35.47)	3.96 (−10.96, 19.07)	0.03 (−0.02, 0.08)
year: year 2021	**−122.09 (−171.88, −72.84)** ***	**-86.63 (−138.86, −34.94)** ***	**−211.50 (−319.03, −105.10)** ***	**−71.94 (−101.90, −42.29)** ***	−0.10 (−0.20, 0.00)
random intercepts					
σ2	2064.50	2816.36	6260.96	899.10	0.01
τ00	0.00 nest	0.00 nest	4446.09 nest	0.00 nest	0.00 nest
	2518.75 TimeMito	2008.35 TimeMito	12184.55 TimeMito	695.27 TimeMito	0.01 TimeMito
N	30 nest	30 nest	30 nest	30 nest	30 nest
	29 TimeMito	29 TimeMito	29 TimeMito	29 TimeMito	29 TimeMito c
observations	49	49	49	49	49

[a]Slope β is given for fixed effects. Confidence intervals (CI) and credible intervals (CrI) not overlapping zero are marked in bold. [b]Significance of fixed effects in the frequentist LMM is given as ***p < 0.001, **p < 0.01, and *p < 0.05. Note that we did not calculate p-values for effects whose CrI overlapped zero. [c]Scaled/centered around the mean.

https://doi.org/10.1021/envhealth.5c00297
Environ. Health 2026, 4, 782−799

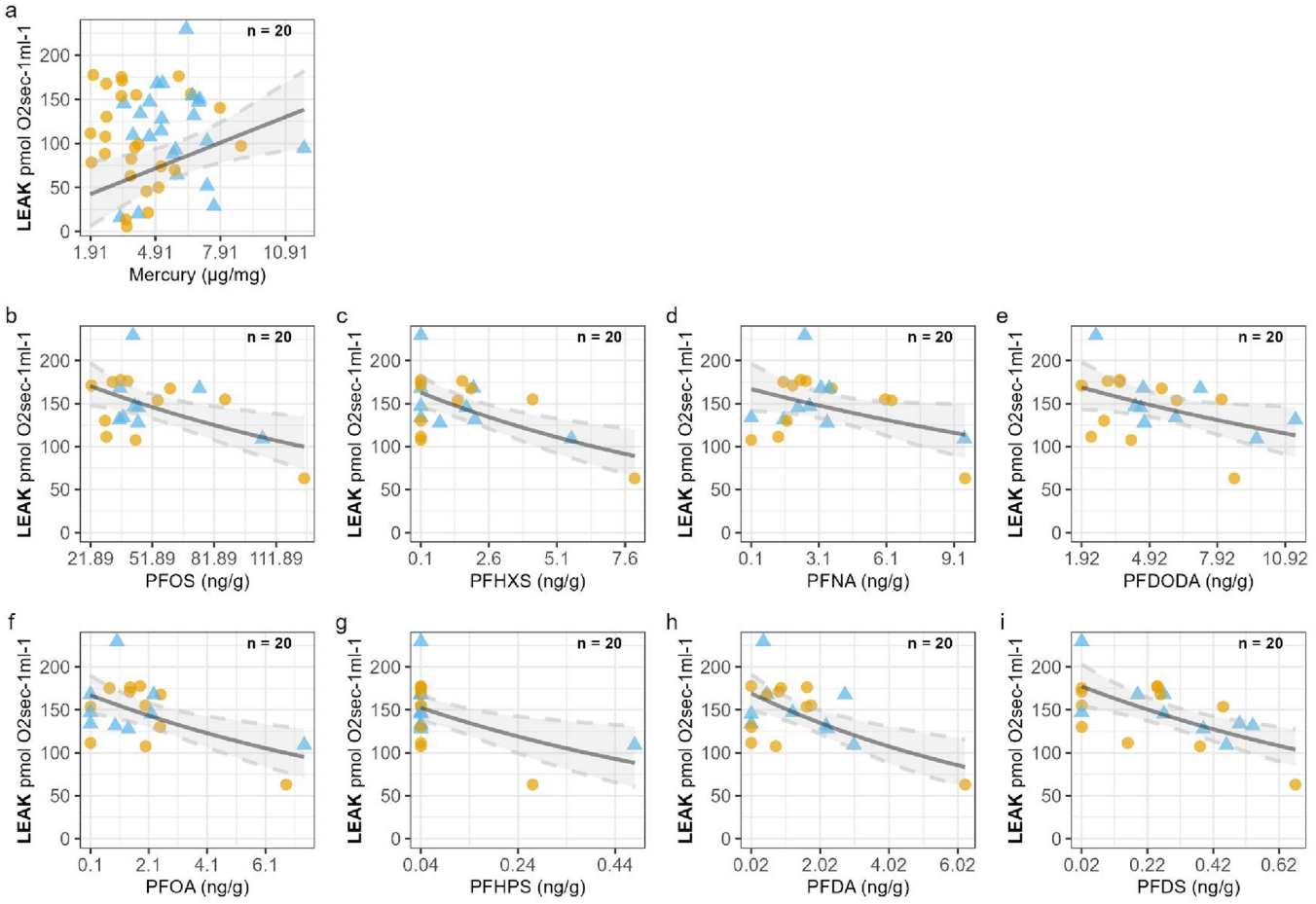

Figure 3. LEAK levels in relation to (a) Mercury (Hg) and (b–i) PFAS in blood samples of Scopoli's shearwaters. A linear mixed-effects model showed that Hg positively associates with LEAK levels. Generalized linear models with a Gamma distribution showed that specific PFAS were negatively associated with LEAK levels. Raw data are shown as semitransparent points in the background. The regression line is shown as a thick line with shaded 95% CrI areas. Female data points are presented in yellow and male in blue.

documented with concentrations of 7.7 ± 3.6 $\mu g g^{-1}$ (range: 2.0–18.7 $\mu g\, g^{-1}$).[53] As expected, Hg concentrations increased in individuals with elevated $\delta^{15}N$ values, which likely indicated a diet richer in predatory fish. This pattern reflects the well-documented biomagnification process across the food web, where Hg concentrations increase in animals that occupy higher trophic levels.[54] Similar relationships have been observed in other seabirds, such as gray-headed albatross[17] and Antarctic petrels.[16] The $\delta^{15}N$ values of Scopoli's shearwaters in our study ranged from 7.42‰ to 9.98‰, indicating some trophic variation, given the commonly assumed enrichment of 3.4‰ per trophic level [39]. This spread likely reflects the species' broad diet, including pelagic fish, crustaceans, and cephalopods,[37,55] whose composition shifts with breeding stages and prey availability.[38,56] The $\delta^{15}N$ range we observed matches values previously reported for shearwaters in the Sicilian channel.[37] On the other hand, the low variation observed in $\delta^{13}C$, falling within the range expected for a single trophic chain, provides limited insight into habitat use in our study. This pattern is likely due to the relatively small geographical scale of the known foraging area used by Scopoli's shearwaters breeding on Linosa during the chick rearing period, which is restricted to the Mediterranean during chick provisioning trips.[13] Although Hg was associated with both $\delta^{15}N$ and $\delta^{13}C$, the evident correlation between $\delta^{13}C$ and $\delta^{15}N$ (Supporting Information; Figure S2), suggests they convey overlapping dietary information. We therefore focused on $\delta^{15}N$ and did not pursue additional analyses linking $\delta^{13}C$ to mitochondrial bioenergetics.

When physiological effects were examined, we found that individuals with higher Hg concentrations showed greater mitochondrial LEAK respiration. In vitro studies have shown that the specific chemical nature of Hg can modify critical proteins in cellular membranes, potentially leading to structural changes that increase mitochondrial permeability and, consequently, proton leakage. This, in turn, may reduce mitochondrial efficiency in coupling oxygen respiration to ATP production. Consistent with our predictions, we observed a higher LEAK with elevated Hg concentrations. However, this did not result in a meaningful change in overall mitochondria inefficiency (FCR_1=LEAK/CMR) because birds up-regulated their oxidative capacity (higher CMR), buffering the immediate costs. Indeed, there was a positive but statistically non-meaningful association between Hg concentrations and CMR (Table 5a and Figure S3, Supporting Information). Such compensation, however, is itself energetically expensive and may not be sustainable in the long term or when additional stressors occur simultaneously or act in similar ways (see below). Higher LEAK values indicate a greater proportion of oxygen consumed by mitochondria that is not used for ATP production, potentially leading to energetic limitations at a whole-organism level. In our population, for example, higher LEAK levels could potentially impact fitness by reducing energy availability for key

https://doi.org/10.1021/envhealth.5c00297
Environ. Health 2026, 4, 782–799

Table 4. Comparison of Linear Mixed-Effects Models: Estimates of the Effect of Σ PFAS (ng g^{-1}) Measured on Mitochondrial Bioenergetic Traits in Blood Samples of Adult Scopoli's Shearwater during Chick Rearing in 2020

	(a) CMR	(b) OXPHOS	(c) ETS	(d) LEAK	(e) FCR_l
(marginal R^2/conditional R^2)	(0.405/0.956)	(0.236/0.567)	(0.078/0.756)	(0.452/0.651)	(0.197/0.197)
fixed effects					
	β (95% CrI)[a] p[b]	β (95% CrI)[a] p[b]	β (95% CrI)[a] p[b]	β (95% CrI)[a] p[b]	β (95% CrI)[a] p[b]
intercept	348.83 (311.58, 388.32) ***	220.83 (184.59, 256.84) ***	503.48 (417.52, 588.60) ***	140.00 (121.03, 158.80) ***	0.38 (0.32, 0.44)
Σ PFAS[c]	−6.91 (−19.91, 5.54)	6.67 (−18.43, 31.43)	1.81 (−45.03, 46.75)	−10.74 (−24.17, 2.48)	−0.03 (−0.08, 0.01)
sex: male	−9.12 (−61.04, 44.09)	−37.67 (−115.22, 41.71)	−20.42 (−140.45, 186.66)	−24.39 (−64.72, 16.74)	0.07 (−0.06, 0.19)
body mass[c]	−0.66 (−32.23, 29.87)	8.25 (−35.29, 50.46)	−1.38 (−96.96, 89.82)	16.67 (−5.80, 38.42)	0.00 (−0.06, 0.07)
age[c]	−59.52 (−105.67, −11.77) *	−44.88 (−86.51, 4.29)	−44.53 (−153.16, 67.85)	−28.82 (−51.64, −5.22) *	0.02 (−0.04, 0.08)
random intercepts					
σ2	270.95	1728.00	4579.62	517.52	0.01
τ00	2862.95 nest	1324.65 nest	11185.99 nest	210.74 nest	0.00 nest
	504.27 TimeMito	0.00 TimeMito c	1535.93 TimeMito	85.01 TimeMito	0.00 TimeMito c
N	14 nest	14 nest	14 nest	14 nest	14 nest
	11 TimeMito c	11 TimeMito	11 TimeMito	11 TimeMito	11 TimeMito
observations	20	20	20	20	20

[a]Slope β is given for fixed effects. Confidence intervals (CI) and credible intervals (CrI) not overlapping zero are marked in bold. [b]Significance of fixed effects in the frequentist LMM is given as ***p < 0.001, **p < 0.01, and *p < 0.05. Note that we did not calculate p-values for effects whose CrI overlapped zero. [c]Scaled/centered around the mean.

activities such as reproduction, foraging, and self-maintenance. Consistent with this view, elevated mitochondrial proton leak has been associated with biomarkers of reduced longevity, both in wildlife exposed to environmental stressors[57] and in experimental systems where DNP-induced uncoupling led to metabolic costs, reduced reproductive output, and decreased immune function,[58] as well as severe health impairments in humans treated with the now-banned uncouplers for weight loss.[59] Our observations come from data collected during the critical chick-rearing phase, when adult shearwaters must ensure the survival of their single-sired offspring. During this period, adults display different foraging strategies to meet both their own energetic needs and those of their chicks.[60] Moreover, Casagrande and Dell'Omo[61] recently showed that shearwater chicks reared at elevated nest temperatures display a ∼20% increase in LEAK relative to normothermic nests. If chicks hatched from Hg-burdened parents inherit or accumulate similar contaminant loads, the two drivers—heat and Hg—are likely to act additively, pushing mitochondrial proton leak beyond the capacity that can be offset by higher CMR. Under Mediterranean heat-wave scenarios, this could translate into slower growth, delayed fledging, or outright chick failure, ultimately depressing annual reproductive success, a possibility that future studies should investigate. Examples of how Hg exposure might affect energy use in wild populations include observed decreases in swimming ability and increased abnormal behavior under stress associated with elevated Hg concentrations in a wild mouse population.[62] Similarly, in little auks, the most abundant Arctic seabird, Hg contamination, though not directly linked to changes in activity budgets, was associated with longer interdive intervals during extended dives, suggesting that Hg imposes physiological limitations on energy use.[63] With climate warming expected to intensify prey fluctuations and heat stress, any contaminant-induced rise in maintenance costs will shrink the "energy margin" available for growth, reproduction, migration, and immune defense. Consequently, Hg exposure at the sublethal level documented here may erode population resilience long before overt mortality is detected, underscoring the need to integrate mechanistic biomarkers such as LEAK into seabird conservation and contaminant-management frameworks. Alternatively, limited prey availability could also be a driver of cell inefficiency. This could be indicated by a shift in diet composition, and future studies could investigate the relationship between fatty acid composition and diet quality in times of food scarcity and the potential effects on the cell or physiology.

We report the mean sum of PFAS in dry weight blood values (details in Supporting Information, Table S1), several times higher than previously documented in incubating adult shearwaters breeding in several colonies across the Mediterranean Sea.[12] These elevated values suggest ongoing exposure of PFAS in the species, despite recent evidence showing a substantial decline in liver PFAS levels in Mediterranean shearwaters over the past 14 years, likely due to stricter regulatory measures.[32] The lipophilic property of PFAS makes them highly likely to adhere to the negatively charged mitochondrial matrix, potentially impacting mitochondrial membrane structure and function.[23] Consequently, we expected the sum of PFAS concentrations to be associated with cellular bioenergetic traits in Scopoli's shearwaters. However, contrary to our expectations, the sum of all measured PFAS appeared to have a negligible role in influencing mitochondrial bioenergetic traits in shearwaters. A plausible explanation is that only a subset

https://doi.org/10.1021/envhealth.5c00297
Environ. Health 2026, 4, 782−799

Table 5. (a) Specific PFAS compounds with Documented In Vitro and In Vivo Effects in Laboratory Studies and Detected in Adult Scopoli's Shearwaters during Chick Rearing Phase. (b) Results from Generalized Linear Models (Gamma Distribution) Assessing Their Effects on Mitochondrial Bioenergetic Traits

(a)				(b)				
abbreviation	full name	mitochondrial effects (*in vitro* and *in vivo*) reported in the literature	detected Conc. (ng/g) in shearwaters (Mean ± SD)	meaningful effect on mitochondria bioenergetic traits in shearwaters (yes or no), β (95% CrI)[a] *p*-value[b], R^2				
				CMR	OXPHOS	ETS	LEAK	FCR_1
PFOS	perfluorooctanesulfonic acid	induces cardiac mitochondrial injury and alters gene transcript expression in pregnant rats[74] induces toxicity in human lymphocytes via oxidative stress and damage to cellular suborganelles[75] causes excessive ROS production and malformations in heart tissue, leading to mitochondrial damage and apoptosis in zebrafish larvae[64]	1.81 ± 1.94	no, −0.002 (−0.005, 0.001), 0.08	no, −0.001 (−0.005, 0.003), 0.01	no, −0.001 (−0.005, −0.003), 0.009	**yes, −0.005 (−0.009, −0.0.001) *, 0.24**	no, −0.002 (−0.005, 0.001), 0.07
PFHxS	perfluorohexanesulfonic acid	exposure leads to cytotoxicity, inhibition of oocyte maturation, and increased mitochondrial membrane potential in pig oocytes[76] treated mice exhibit reproductive toxicity, including decreased sperm count and mobility, along with dysregulated expression of mitochondrial biogenesis proteins[77]	1.45 ± 2.10	no, −0.037 (−0.077, 0.007), 0.10	no, −0.01, (−0.069, 0.045), 0.00	no, −0.019 (−0.069, 0.032), 0.02	**yes, −0.076 (−0.125, −0.31) *, 0.33**	no, −0.036 (−0.080, 0.006), 0.12
PFNA	perfluorononanoic acid	impairs oocyte maturation in mice by inducing mitochondrial dysfunction (abnormal distribution, increased mitochondrial membrane potential) and ROS production, leading to oxidative stress[78]	3.20 ± 2.61	no, −0.018 (−0.049, 0.016), 0.03	no, −0.005 (−0.050, 0.043), 0.00	no, −0.009 (−0.048, 0.035), 0.00	**yes, −0.039 (−0.080, −0.001) *, 0.14**	no, −0.02 (−0.057, 0.013), 0.06
PFDODA	perfluorododecanoic acid	structurally similar to PFUnA; no studies available	5.13 ± 2.58	no, −0.019 (−0.055, 0.015), 0.05	no, −0.004 (−0.056, 0.044), 0.00	no, −0.00 (−0.045, 0.038), 0.00	**yes, −0.043 (−0.081, −0.005) **, 0.18**	no, −0.019 (−0.056, 0.016), 0.06
PFOA	perfluorooctanoic acid	mitochondrial and lipid metabolism effects: exposure in mice results in mitochondrial dysfunction, increased ROS, and DNA damage, impairing oocyte maturation[65,79] in zebrafish, PFOA leads to premature ovarian insufficiency by impairing NAD+ synthesis and mitochondrial function[66]	1.81 ± 1.94	no, 0.015 (−0.043, 0.077), 0.02	no, 0.015 (−0.043, 0.077), 0.01	no, 0.004 (−0.054, 0.059), 0.00	**yes, −0.054 (−0.099, −0.012) *, 0.024**	**yes, −0.053 (−0.098, −0.009)*, 0.24**
PFHPS	perfluoroheptanesulfonic acid	no studies available	0.17 ± 1.10	no, −0.236 (−1.049, 0.661), 0.01	no, 0.292 (−0.822, 1.398), 0.01	no, 0.016 (−0.974, 1.059), 0.00	**yes, −1.250 (−2.161, −0.327) *, 0.26**	**yes, −1.017 (−1.826, −0.194) *, 0.24**
PFDA	perfluorodecanoic acid	similar to PFNA; evidence of mitochondrial toxicity in isolated rat liver mitochondria, increasing PFDA concentrations (87.5 μg mL^{-1}) caused a linear increase in oxygen consumption during nonphosphorylating respiration, suggesting uncoupling of electron transport (ETS) and OXPHOS. Higher doses (>87.5 μg mL^{-1}) progressively reduced state 4 oxygen consumption, and at 150 μg mL^{-1}, state 3 respiration was completely inhibited[24]	1.26 ± 1.48	**yes, −0.07 (−0.14, −0.01) *, 0.21**	No, −0.05 (−0.139, 0.026), 0.06	No −0.061 (−0.135, 0.005), 0.09	**Yes, −0.116 (−0.180, −0.052)**, 0.34**	No, −0.028 (−0.099, 0.038),
PFDS	perfluorodecanesulfonic acid	structurally similar to PFOS but less studied; no available studies	0.24 ± 0.20	**yes, −0.672 (−1.067, 0.253)**, 0.31**	no, −0.550 (−1.150, 0.095), 0.12	**yes, −0.555 (−1.152, −0.066)*, 0.16**	**yes, −0.811 (−1.269, −0.377)**, 0.38**	no, −0.837 (−0.610, 0.434), 0.00
PFOSA	perfluorooctane sulfonamide	induces ROS overproduction, mitochondrial membrane potential collapse, and apoptosis in zebrafish larvae hearts[64]	3.84 ± 2.25	no, 0.003 (−0.03, 0.041), 0.00	no, 0.021 (−0.024, 0.064), 0.02	no, −0.01 (−0.031, 0.053), 0.01	no, −0.018 (−0.063, 0.024), 0.03	no, −0.02 (−0.060, 0.016), 0.07
PFTriDA	perfluorotridecanoic acid	no studies available	7.20 ± 4.86	no, −0.002 (−0.020, 0.0176). 0.00	no, −0.000 (−0.027, 0.022), 0.00	no, 0.002 (−0.019, 0.026), 0.00	no, −0.004 (−0.025, 0.016), 0.00	no, −0.001 (−0.018, 0.020), 0.00

https://doi.org/10.1021/envhealth.5c00297
Environ. Health 2026, 4, 782−799

Table 5. continued

(a)				(b)				
abbreviation	full name	mitochondrial effects (*in vitro* and *in vivo*) reported in the literature	detected Conc. (ng/g) in shearwaters (Mean ± SD)	meaningful effect on mitochondria bioenergetic traits in shearwaters (yes or no), β (95% CrI)[a] *p*-value[b], R^2				
				CMR	OXPHOS	ETS	LEAK	FCR_1
PFUnA	perfluoroundecanoic acid	no studies available	13.49 ± 5.88	no, −0.008 (−0.024, 0.006), 0.04	no, −0.003 (−0.024, 0.018), 0.00	no, −0.002 (−0.020, 0.016), 0.00	no, −0.017 (−0.0355, 0.000), 0.14	no, −0.007 (−0.0248, 0.009), 0.03
PFTDA	perfluorotetradecanoic acid	no studies available	1.97 ± 1.22	no, 0.005 (−0.065, 0.081), 0.00	no, 0.028 (−0.068, 0.122), 0.01	no, 0.028 (−0.06,1, 0.115), 0.01	no, −0.02 (−0.113, 0.056), 0.02	no, −0.041 (−0.121, 0.03), 0.05
P37DMOA	perfluoro-3,7-dimethyloctanoic acid	no studies available	0.02 ± 0.04	no, 0.964 (−1.08, 3.166), 0.04	no, 1.035 (−1.848, 4.05), 0.02	no, 0.450 (−1.965, 3.045), 0.00	no, 0.909 (−1.651, 3.29), 0.03	no, −0.136 (−2.296, 2.069), 0.00
10:2 FTS	1H,2H-perfluorododecan sulfonate (10:2)	no studies available	1.07 ± 1.11	no, 0.013 (−0.068, 0.097), 0.00	no, 0.027 (−0.087, 0.133), 0.00	no, 0.016 (−0.085, 0.108), 0.00	no, −0.004 (−0.103, 0.096), 0.00	no, −0.000 (−0.096, 0.084), 0.00

[a]Slope β is given for predictors. Confidence intervals (CI) and credible intervals (CrI) not overlapping zero are marked in bold. [b]Significance of predictors in the frequentist GLM (Gamma distribution) are given as ***$p < 0.001$, **$p < 0.01$, and *$p < 0.05$. Note that we did not calculate *p*-values for effects whose CrI overlapped zero.

https://doi.org/10.1021/envhealth.5c00297
Environ. Health 2026, 4, 782−799

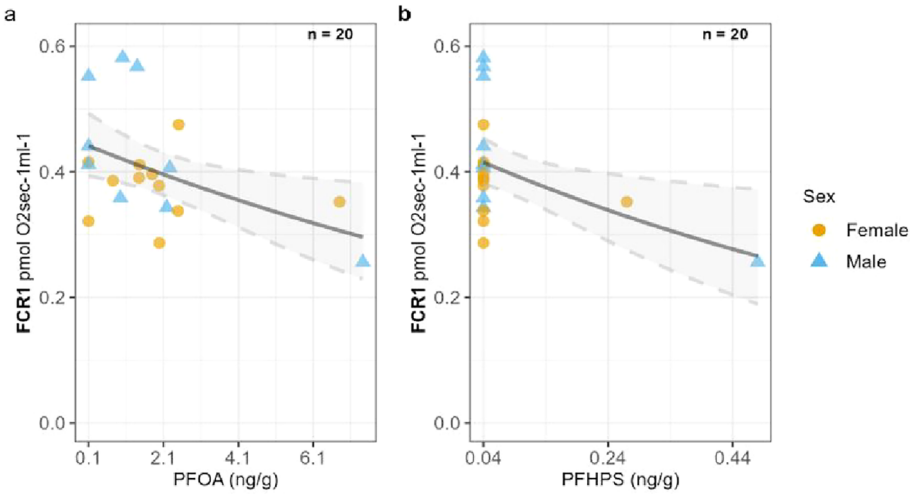

Figure 4. FCR_l levels in relation to specific PFAS detected in blood samples of Scopoli's shearwaters during chick rearing. Generalized linear models with a Gamma distribution showed that specific PFAS negatively associate with FCR_l levels. Raw data are shown as semitransparent points in the background. The regression line is shown as a thick line with shaded 95% CrI areas. Female data points are presented in yellow and male in blue.

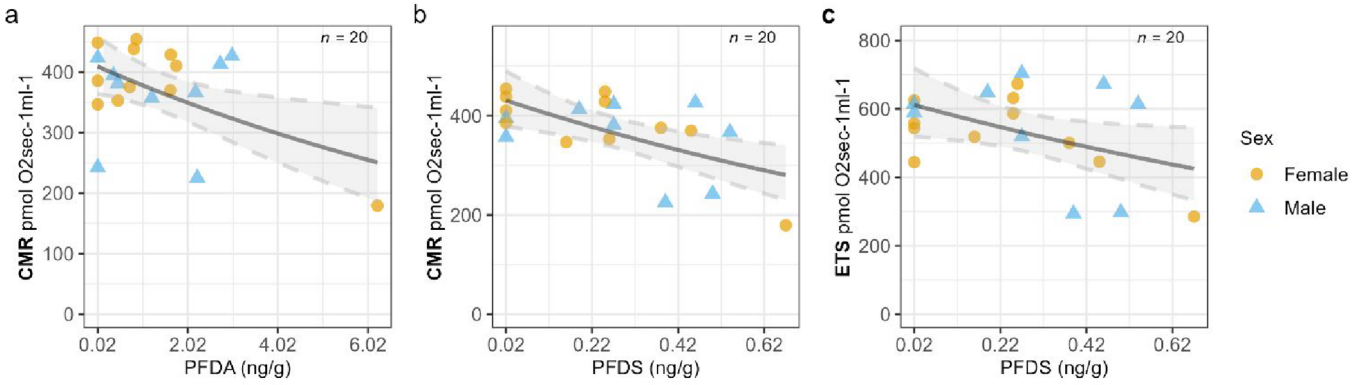

Figure 5. Mitochondrial bioenergetic traits (a, b) CMR and (c) ETS levels in relation to specific PFAS detected in blood samples of Scopoli's shearwaters during chick-rearing. Generalized linear models with a Gamma distribution showed that specific PFAS negatively associate with CMR levels. Raw data are shown as semitransparent points in the background. The regression line is shown as a thick line with shaded 95% CrI areas. Female data points are presented in yellow and male in blue.

of congeners actually interfere with mitochondrial function (see Table 5 for specific PFAS effects reported in the literature). When we analyzed single PFAS congeners, several displayed a strong negative association with LEAK respiration and the LEAK-to-CMR ratio (FCR_l), which was in accordance with our prediction. Similar but weaker associations were occasionally observed for CMR and ETS, suggesting that LEAK and FCR_l are the primary mitochondrial targets of PFAS in this species. This pattern aligns with findings from laboratory studies (Table 5a). PFAS are known to increase oxidative stress by enhancing mitochondrial membrane potential.[64−66] Under normal physiological conditions, LEAK respiration is upregulated in response to elevated ROS levels as a protective feedback mechanism to reduce the proton gradient, thereby limiting further ROS production. Our findings in Scopoli's shearwaters suggest that higher concentrations of specific PFAS compounds are associated with lower LEAK respiration, potentially impairing this regulatory feedback loop. This disruption is consistent with the idea that PFAS interfere with mitochondrial responses to oxidative stress, potentially compromising cellular protection mechanisms.[64−66] Such impairment aligns with predictions of the "uncoupling-to-survive" hypothesis, whereby reduced LEAK may reflect a failure to activate protective uncoupling in the face of ROS, rather than an improved mitochondrial efficiency.

Beyond mitochondrial effects, PFAS are known to interfere with hormonal systems regulating metabolism and body condition in sea birds.[67] For example, in the black-legged kittiwake (*Rissa tridactyla*), PFAS were associated with altered circulating levels of thyroid hormones and sex-specific associations with body mass.[67] Yet, in our study population, these physiological adjustments did not translate into measurable changes in body mass (see Table S2 for the Supporting Information for specific models). Interestingly, these trends were observed during the chick-rearing phase, when PFAS concentrations in this population are lower compared to incubation,[13] raising the possibility that prior exposure during incubation may have also played a role. Understanding whether PFAS-induced suppression of LEAK is a reversible response or progressive is essential for assessing long-term impacts on seabird energetic physiology and has direct conservation value. Long-term monitoring that couples serial bioenergetic profiling with survival and reproductive metrics will be essential to gauge colony-level risk and to inform regulatory thresholds for PFAS in marine ecosystems. Especially in the context of temporal and spatial variability in pollutant exposure, which can occur over

https://doi.org/10.1021/envhealth.5c00297
Environ. Health 2026, 4, 782−799

Table 6. Comparison of Linear Mixed-Effects Models: Estimates of the Effect of $\delta^{15}N$ and $\delta^{13}C$ in Blood Samples of Adult Scopoli's Shearwater on Mitochondrial Bioenergetic Traits

	(a) **CMR**	(b) **OXPHOS**	(c) **ETS**	(d) **LEAK**	(e) **FCR_1**
(marginal R^2/conditional R^2)	(0.378/0.716)	(0.246/0.606)	(0.246/0.777)	(0.494/0.674)	(0.262/0.479)
fixed effects					
	β (95% CrI)[a] p[b]	β (95% CrI)[a] p[b]	β (95% CrI)[a] p[b]	β (95% CrI)[a] p[b]	β (95% CrI)[a] p[b]
intercept	**405.57 (331.15, 479.79)** ***	**220.72 (−179.59, 260.93)** ***	**513.07 (423.96, 599.99)** ***	**151.13 (129.52, 172.19)** ***	0.41 (0.33, 0.49) ***
$\delta^{15}N$[c]	10.79 (−7.87, 29.61)	−4.24 (−16.27, 24.94)	13.23 (−26.39, 52.97)	**20.71 (9.29, 32.18)** **	**0.06 (0.02, 0.11)** **
sex: male	3.33 (−41.28, 49.20)	5.61 (−43.39, 55.84)	10.79 (−80.01, 104.39)	−14.24 (−41.46, 13.64)	−0.03 (−0.13, 0.07)
age[c]	−3.25 (−9.51, 3.10)	−14.65 (−37.57, 8.48)	−6.28 (−18.46, 5.93)	−6.47 (−18.47, 5.71)	0.01 (−0.04, 0.05)
bodymass[c]	−23.20 (−47.38, 0.85)	−15.26 (−41.71, 10.95)	−13.21 (−65.06, 38.60)	2.98 (−11.41, 17.21)	0.03 (−0.03, 0.08)
year: year 2021	**−112.65 (−160.46, −65.35)** ***	**−78.66 (−129.65, −28.20)** ***	**−63.66 (−90.70, −36.91)** ***	**−65.32 (−92.22, −37.52)** ***	−0.08 (−0.18, 0.01)
random intercepts					
σ2	2120.55	2673.36	7056.83	894.02	0.01
τ00	0.00 nest	0.00 nest	4371.68 nest	0.00 nest	0.00 nest
	2529.65 TimeMito	2445.96 TimeMito	12489.67 TimeMito	496.44 TimeMito	0.00 TimeMito
N	30 nest	30 nest	30 nest	30 nest	30 nest
	29 TimeMito	29 TimeMito	29 TimeMito	29 TimeMito	29 TimeMito
observations	49	49	49	49	49

[a]Slope β is given for fixed effects. Confidence intervals (CI) and credible intervals (CrI) not overlapping zero are marked in bold. [b]Significance of fixed effects in the frequentist LMM is given as ***p < 0.001, **p < 0.01, and *p < 0.05. Note that we did not calculate p-values for effects whose CrI overlapped zero. [c]Scaled/centered around the mean.

https://doi.org/10.1021/envhealth.5c00297
Environ. Health 2026, 4, 782−799

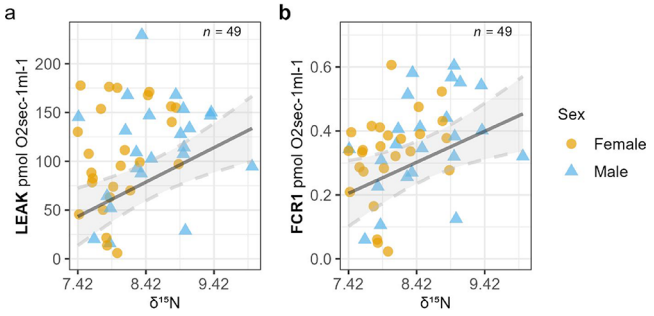

Figure 6. Mitochondrial bioenergetic traits in Scopoli's shearwaters in relation to trophic position (δ^{15}N). A linear mixed-effect model showed that δ^{15}C was positively correlated with (a) LEAK and (b) FCR_l values. Raw data are shown as semitransparent points in the background. The regression line is shown a thick line with shaded 95% CrI areas. Female data points are presented in yellow and male in blue.

relatively small scales. For instance, blood concentrations of PFAS can reflect local exposure differences[13] and reveal crucial stages for depuration processes.

Contaminant levels were linked to individual traits only in the case of Hg: males showed higher Hg concentrations than females, whereas total PFAS concentrations showed no such difference. This observation aligns with known patterns where females excrete Hg through egg laying[33,68] and sexual differences in foraging ecology contribute to variations in Hg burdens.[69] We also observed a trend of higher Hg concentrations in older individuals, likely reflecting the bioaccumulation of Hg in the body over time. This pattern contrasts with previous avian studies[70] that did not find an age effect and highlighted that Hg can be depurated in the feathers at each feather molt. Importantly, Hg-age association seems to be independent of body mass, which was not meaningfully associated with Hg concentrations in our study. These findings are consistent with a recent meta-analysis in birds, which concluded that body condition is a poor predictor of sublethal Hg exposure,[71] where contaminant loads track age rather than morphological variation. The alignment of our findings with previously established associations between Hg concentrations and individual traits or foraging habits highlights the robustness of our data set in examining the relationship between Hg exposure and mitochondrial bioenergetic processes.

Our results also revealed distinct relationships between isotopic signatures and mitochondrial function: δ^{15}N was positively associated with higher LEAK and FCR_l levels, indicating a reduced coupling efficiency of mitochondria with ATP production in individuals occupying higher trophic positions. While predatory fish are an essential component of the natural diet of shearwaters, in some contexts, they have the potential to become a suboptimal component influencing their cellular energetic metabolism (i.e., "the junk food hypothesis"[72]). This is primarily because, compared to other prey, fish are more likely to accumulate environmental pollutants such as Hg or persistent organic pollutants (POPs).[2,5] Scopoli's shearwaters also forage near fishing vessels and exploit fish discards,[38,56] which might constitute a suboptimal food source likely due to low energy content and poor nutritional quality, as shown in Northern gannets.[73] Fish discards can consist of parts of fish that are less nutrient-dense compared to prey shearwaters naturally hunt, particularly during the breeding period, such as small pelagic fish[37] (e.g., anchovies, sardines, etc.), which are of higher nutritional value. These discards might also lack sufficient high-quality proteins, essential fatty acids, and micronutrients as a result of decomposing processes during exposure on fish vessels before discard. Moreover, we observed that Scopoli's shearwaters at higher trophic positions, indicated by higher δ^{15}N values, were also more exposed to Hg, which could explain, even alone, the association with increased proton leak and mitochondrial inefficiency. This suggests that the effects of the trophic position on mitochondrial bioenergetics may be mediated by Hg exposure. Future research should experimentally explore how dietary quality interacts with contaminant exposure to influence mitochondrial functions.

5. CONCLUSIONS

Our study provides novel insights into the relationships between contaminant levels and mitochondrial bioenergetics in the wild seabird population. We demonstrated that Hg levels in shearwaters, also influenced by their trophic level position, are associated with mitochondrial proton leakage, suggesting a link between Hg exposure and mitochondrial inefficiency in producing ATP. This highlights the potential physiological implications of Hg-contaminant exposure, particularly in species with intensive energetic demands such as shearwaters during breeding. In contrast, we found no associations between the summed PFAS levels and mitochondrial bioenergetic traits. However, we did observe associations with specific PFAS concentrations despite the limitations of our data set sample size, which may also reflect differences in the biological and time-dependent pathways affected by PFAS compared to Hg. Because the mitochondrial membrane potential was not directly measured, the mechanistic basis of these effects remains uncertain. Future work incorporating independent assessments of membrane potential will be essential to clarify how xenochemical exposure alters mitochondrial function. Future studies should also aim to directly link mitochondrial function with individual fitness outcomes, for instance, through long-term monitoring of reproductive success and survival, to test whether the energetic costs associated with LEAK perturbation translate into population-level consequences. These findings emphasize the need for further research to disentangle the mechanisms by which contaminants influence mitochondrial function, particularly in long-lived species and apex predators that are vulnerable to contaminant exposure. Future studies incorporating longitudinal data and broader spatial and temporal scales will be crucial for understanding how foraging patterns, contaminant exposure, and mitochondrial bioenergetics interact to shape the fitness of wild populations in increasingly anthropogenically altered environments.

■ ASSOCIATED CONTENT

Data Availability Statement

The data analysis script, written in R, along with the associated data set, is available on GitHub https://github.com/lguadal/ContaminantsMitoShearwaters. The full data set is public and accessible to ensure transparency and reproducibility of our results.

Supporting Information

The Supporting Information is available free of charge at https://pubs.acs.org/doi/10.1021/envhealth.5c00297.

Statistical analysis. Table S1, Table S2, Figure S1, Figure S2, Figure S3 (PDF)

https://doi.org/10.1021/envhealth.5c00297
Environ. Health 2026, 4, 782−799

AUTHOR INFORMATION

Corresponding Author

Stefania Casagrande − *Evolutionary Physiology Research Group, Max Planck Institute for Biological Intelligence, Seewiesen 82319, Germany;* orcid.org/0000-0002-4264-8062; Email: Stefania.Casagrande@bi.mpg.de

Authors

Guadalupe Lopez-Nava − *Evolutionary Physiology Research Group, Max Planck Institute for Biological Intelligence, Seewiesen 82319, Germany;* orcid.org/0009-0008-8288-9486

Lucie Michel − *Animal Ecology and Systematics, Justus-Liebig University, Giessen 35390, Germany*

Giacomo Dell'Omo − *Ornis italica, Rome 00199, Italy*

Petra Quillfeldt − *Animal Ecology and Systematics, Justus-Liebig University, Giessen 35390, Germany*

Paco Bustamante − *Littoral Environnement et Sociétés (LIENSs), La Rochelle 17000, France*

Complete contact information is available at: https://pubs.acs.org/10.1021/envhealth.5c00297

Author Contributions

G.L.-N. and L.M. contributed equally to this work. L.M. and S.C. conceived the study, collected and curated the data, and conducted the literature review. G.D. assisted with field data collection. S.C. conducted the mitochondrial bioenergetics analyses. L.M. and P.B. performed the elemental analyses. L.M. performed the PFAS analysis. G.L.-N. conducted the formal data analyses, performed a literature review, and wrote the original draft of the manuscript together with S.C. and L.M. G.D., P.B., and P.Q. contributed to conceptual input, critical review of results, and manuscript editing. All authors read and approved the final version.

Funding

L.M. was supported by a Ph.D. project financed by a Deutsche Forschungsgemeinschaft (DFG) grant QU 148/23 to P. Quillfeldt from the University of Giessen. G.L.-N. was supported by the IMPRS (International Max Planck Research School). S.C. was supported by the Max Planck Society (MPG). Thanks are due to the CPER (Contrat de Projet Etat-Région) and the FEDER (Fonds Européen de Développement Régional) for funding the IRMSs of LIENSs laboratory.

Notes

All the experimental procedures described in the study were granted by the authorities of Regione Sicilia (protocol no. 24156) and approved by Istituto Superiore per la Protezione e Ricerca Ambientale (ISPRA, protocol no. 24065).
The authors declare no competing financial interest.

ACKNOWLEDGMENTS

We thank our collaborators from the scientific association Ornis Italica—especially Eleonora Dell'Omo, Vittoria Roatti, Marco Cianchetti, Antonella Di Gangi, and Dario D'Emanuele—for the long-term monitoring program on the Scopoli's shearwater population. We are grateful to the Evolutionary Physiology Research Group at the Max Planck Institute for Biological Intelligence for their valuable feedback on the data, especially Michaela Hau, whose support was instrumental in carrying out this research. We want to thank Prof. Dr. Veerle L.B. Jaspers from the Department of Biology at NTNU Trondheim for providing the analytical expertise and hosting a laboratory placement, as well as Prof. Dr. Alexandros Asimakopoulos and Dr. Junjie Zhang from the Department of Chemistry at NTNU Trondheim for providing their infrastructure for the PFAS analysis. We are grateful to C. Churlaud and M. Brault-Favrou from the platform Analyses Elémentaires of LIENSs for their assistance during Hg analysis and to G. Guillou from the platform Analyses isotopiques of LIENSs for running the stable isotope analyses. Thanks are due to the CPER (Contrat de Projet Etat-Région) and the FEDER (Fonds Européen de Développement Régional) for funding the AMA and IRMS of LIENSs laboratory. PB is an honorary member of the IUF (Institut Universitaire de France).

ABBREVIATIONS

Hg, Mercury; PFAS, Per- and Polyfluoroalkyl Substances; CMR, Cellular Metabolic Rate (baseline); OXPHOS, Oxidative Phosphorylation; ETS, Electron Transport System; LEAK, Mitochondrial Proton Leak; FCR_1, Mitochondrial Inefficiency (ratio Leak CMR^{-1}); PFOS, Perfluorooctanesulfonic Acid; PFHxS, Perfluorohexanesulfonic Acid; PFNA, Perfluorononanoic Acid; PFDODA, Perfluorododecanoic Acid; PFOA, Perfluorooctanoic Acid; PFHPS, Perfluoroheptanesulfonic Acid; PFDA, Perfluorodecanoic Acid; PFDS, Perfluorodecanesulfonic Acid; PFOSA, Perfluorooctane Sulfonamide; PFTRIDA, Perfluorotridecanoic Acid; PFUNA, Perfluoroundecanoic Acid; PFTDA, Perfluorotetradecanoic Acid; P37DMOA, Perfluoro-3,7-dimethyloctanoic Acid; FTS_10_2, Perfluoro-1-decylsulfonic Acid

REFERENCES

(1) Duarte, C.; Chapuis, L.; Collin, S.; Costa, D.; Devassy, R.; Eguíluz, V.; Erbe, C.; Gordon, T.; Halpern, B.; Harding, H.; Havlik, M.-N.; Meekan, M.; Merchant, N.; Miksis-Olds, J.; Parsons, M.; Predragovic, M.; Radford, A.; Radford, C.; Simpson, S.; Slabbekoorn, H.; Staaterman, E.; Van Opzeeland, I.; Winderen, J.; Zhang, X.; Juanes, F. The Soundscape of the Anthropocene Ocean. *Science* **2021**, *371*, No. eaba4658.

(2) Landrigan, P.; Stegeman, J.; Fleming, L.; Allemand, D.; Anderson, D.; Backer, L.; Brucker-Davis, F.; Chevalier, N.; Corra, L.; Czerucka, D.; Bottein, M.; Demeneix, B.; Depledge, M.; Deheyn, D.; Dorman, C.; Fénichel, P.; Fisher, S.; Gaill, F.; Galgani, F.; Gaze, W.; Giuliano, L.; Grandjean, P.; Hahn, M.; Hamdoun, A.; Hess, P.; Judson, B.; Laborde, A.; McGlade, J.; Mu, J.; Mustapha, A.; Neira, M.; Noble, R.; Pedrotti, M.; Reddy, C.; Rocklöv, J.; Scharler, U.; Shanmugam, H.; Taghian, G.; van de Water, J.; Vezzulli, L.; Weihe, P.; Zeka, A.; Raps, H.; Rampal, P. Human Health and Ocean Pollution. *Ann. Glob. Health* **2020**, *86* (1), 151.

(3) Liu, M.; Zhang, Q.; Maavara, T.; Liu, S.; Wang, X.; Raymond, P. A. Rivers as the Largest Source of Mercury to Coastal Oceans Worldwide. *Nature Geoscience* **2021**, *14* (9), 672−677.

(4) Savoca, M.; Robuck, A.; Cashman, M.; Cantwell, M.; Agvent, L.; Wiley, D.; Rice, R.; Todd, S.; Hunter, N.; Robbins, J.; Goldbogen, J.; Lohmann, R. Whale Baleen to Monitor Per- and Polyfluoroalkyl Substances (PFAS) in Marine Environments. *Environmental Science and Technology Letters* **2024**, *11* (8), 862−870.

(5) Singh, M.; Kanaoujiya, R.; Shekhar Srivastava, M. Mercury Impact on Wildlife: An Analysis of the Literature. *Mater. Today Proc.* **2024**, *106*, 84−88.

(6) Lukić Bilela, L.; Matijošytė, I.; Krutkevičius, J.; Alexandrino, D. A. M.; Safarik, I.; Burlakovs, J.; Gaudêncio, S. P.; Carvalho, M. F. Impact of Per- and Polyfluorinated Alkyl Substances (PFAS) on the Marine Environment: Raising Awareness, Challenges, Legislation, and Mitigation Approaches under the One Health Concept. *Mar. Pollut. Bull.* **2023**, *194*, No. 115309.

(7) Gworek, B.; Bemowska-Kałabun, O.; Kijeńska, M.; Wrzosek-Jakubowska, J. Mercury in Marine and Oceanic Waters—a Review. *Water, Air, & Soil Pollution* **2016**, *227* (10), 371.
(8) Zheng, N.; Wang, S.; Dong, W.; Hua, X.; Li, Y.; Song, X.; Chu, Q.; Hou, S.; Li, Y. The Toxicological Effects of Mercury Exposure in Marine Fish. *Bull. Environ. Contam. Toxicol.* **2019**, *102* (5), 714−720.
(9) Qiu, X.; Liu, M.; Zhang, Y.; Zhang, Q.; Lin, H.; Cai, X.; Li, J.; Dai, R.; Zheng, S.; Wang, J.; Zhu, Y.; Shen, H.; Shen, G.; Wang, X.; Tao, S. Declines in Anthropogenic Mercury Emissions in the Global North and China Offset by the Global South. *Nat. Commun.* **2025**, *16* (1), 1179.
(10) Wee, S. Y.; Aris, A. Z. Environmental Impacts, Exposure Pathways, and Health Effects of PFOA and PFOS. *Ecotoxicology and Environmental Safety* **2023**, *267*, No. 115663.
(11) Cherel, Y.; Barbraud, C.; Lahournat, M.; Jaeger, A.; Jaquemet, S.; Wanless, R.; Phillips, R.; Thompson, D.; Bustamante, P. Accumulate or Eliminate? Seasonal Mercury Dynamics in Albatrosses, the Most Contaminated Family of Birds. *Environmental pollution* **2018**, *241*, 124−135.
(12) Escoruela, J.; Garreta, E.; Ramos, R.; González-Solís, J.; Lacorte, S. Occurrence of Per- and Polyfluoroalkyl Substances in Calonectris shearwaters Breeding along the Mediterranean and Atlantic Colonies. *Mar. Pollut. Bull.* **2018**, *131*, 335−340.
(13) Michel, L.; Zhang, J.; Asimakopoulos, A.; Austad, M.; Bustamante, P.; Cecere, J. G.; Cianchetti-Benedetti, M.; Colominas-Ciuró, R.; Dell'Omo, G.; De Pascalis, F.; Jaspers, V. L. B.; Quillfeldt, P. Assessing Perfluoroalkyl Substance Pollution in Central Mediterranean Breeding shearwaters. *Environ. Toxicol. Chem.* **2025**, *44*, 420.
(14) Sebastiano, M.; Jouanneau, W.; Blévin, P.; Angelier, F.; Parenteau, C.; Pallud, M.; Ribout, C.; Gernigon, J.; Lemesle, J. C.; Robin, F.; Pardon, P.; Budzinski, H.; Labadie, P.; Chastel, O. Physiological Effects of PFAS Exposure in Seabird Chicks: A Multi-Species Study of Thyroid Hormone Triiodothyronine, Body Condition and Telomere Length in South Western France. *Science of The Total Environment* **2023**, *901*, No. 165920.
(15) Humann-Guilleminot, S.; Blévin, P.; Gabrielsen, G. W.; Herzke, D.; Nikiforov, V. A.; Jouanneau, W.; Moe, B.; Parenteau, C.; Helfenstein, F.; Chastel, O. PFAS Exposure Is Associated with a Lower Spermatic Quality in an Arctic Seabird. *Environ. Sci. Technol.* **2024**, *58* (44), 19617−19626.
(16) Carravieri, A.; Fort, J.; Tarroux, A.; Cherel, Y.; Love, O. P.; Prieur, S.; Brault-Favrou, M.; Bustamante, P.; Descamps, S. Mercury Exposure and Short-Term Consequences on Physiology and Reproduction in Antarctic Petrels. *Environ. Pollut.* **2018**, *237*, 824−831.
(17) Mills, W. F.; Bustamante, P.; McGill, R. A. R.; Anderson, O. R. J.; Bearhop, S.; Cherel, Y.; Votier, S. C.; Phillips, R. A. Mercury Exposure in an Endangered Seabird: Long-Term Changes and Relationships with Trophic Ecology and Breeding Success. *Proc. R. Soc. B Biol. Sci.* **1941**, *2020* (287), 20202683.
(18) Koch, R. E.; Buchanan, K. L.; Casagrande, S.; Crino, O.; Dowling, D. K.; Hill, G. E.; Hood, W. R.; McKenzie, M.; Mariette, M. M.; Noble, D. W. A.; Pavlova, A.; Seebacher, F.; Sunnucks, P.; Udino, E.; White, C. R.; Salin, K.; Stier, A. Integrating Mitochondrial Aerobic Metabolism into Ecology and Evolution. *Trends in Ecology & Evolution* **2021**, *36* (4), 321−332.
(19) Notariale, R.; Längst, E.; Perrone, P.; Crettaz, D.; Prudent, M.; Manna, C. Effect of Mercury on Membrane Proteins, Anionic Transport and Cell Morphology in Human Erythrocytes. *Cell. Physiol. Biochem.* **2022**, *56* (5), 500−513.
(20) Ji, X.-L.; Wang, W.-H.; Cheng, J.; Yuan, T.; Zhao, X.; Zhuang, H.; Qu, L.-Y. Free Radicals and Antioxidant Status in Rat Liver after Dietary Exposure of Environmental Mercury. *Environmental Toxicology and Pharmacology* **2006**, *22* (3), 309−314.
(21) Belyaeva, E. A.; Sokolova, T. V.; Emelyanova, L. V.; Zakharova, I. O. Mitochondrial Electron Transport Chain in Heavy Metal-Induced Neurotoxicity: Effects of Cadmium, Mercury, and Copper. *Sci. World J.* **2012**, *2012* (1), No. 136063.
(22) Brookes, P. S. Mitochondrial H+ Leak and ROS Generation: An Odd Couple. *Free Radical Biol. Med.* **2005**, *38* (1), 12−23.
(23) Meyer, J. N.; Leung, M. C. K.; Rooney, J. P.; Sendoel, A.; Hengartner, M. O.; Kisby, G. E.; Bess, A. S. Mitochondria as a Target of Environmental Toxicants. *Toxicol. Sci.* **2013**, *134* (1), 1−17.
(24) Langley, A. Effects of Perfluoro-N-Decanoic Acid on the Respiratory Activity Pf Isolated Rat-Liver Mitochondria. *Journal of Toxicology and Environmental Health* **1990**, *29* (3), 329−336.
(25) Liu, Y.; Liu, S.; Huang, J.; Liu, Y.; Wang, Q.; Chen, J.; Sun, L.; Tu, W. Mitochondrial Dysfunction in Metabolic Disorders Induced by Per- and Polyfluoroalkyl Substance Mixtures in Zebrafish Larvae. *Environ. Int.* **2023**, *176*, No. 107977.
(26) Casagrande, S.; Dzialo, M.; Trost, L.; Malkoc, K.; Sadowska, E. T.; Hau, M.; Pierce, B.; McWilliams, S.; Bauchinger, U. Mitochondrial Metabolism in Blood More Reliably Predicts Whole-Animal Energy Needs Compared to Other Tissues. *iScience* **2023**, *26* (12), No. 108321.
(27) Malkoc, K.; Casagrande, S.; Hau, M. Inferring Whole-Organism Metabolic Rate From Red Blood Cells in Birds. *Front. Physiol.* **2021**, *12*, No. 691633.
(28) Tyrrell, D. J.; Bharadwaj, M. S.; Jorgensen, M. J.; Register, T. C.; Shively, C.; Andrews, R. N.; Neth, B.; Dirk Keene, C.; Mintz, A.; Craft, S.; Molina, A. J. A. Blood-Based bioenergetic Profiling Reflects Differences in Brain Bioenergetics and Metabolism. *Oxidative Medicine and Cellular Longevity* **2017**, *2017*, No. 7317251.
(29) Wilkinson, M. S.; Dunham-Snary, K. J. Blood-Based Bioenergetics: A Liquid Biopsy of Mitochondrial Dysfunction in Disease. *Trends in Endocrinology & Metabolism* **2023**, *34* (9), 554−570.
(30) United Nations Environment Programme (UNEP). *Minamata Convention on Mercury*; United Nations Environment Programme: 2013.
(31) Cossa, D.; Knoery, J.; Banaru, D.; Harmelin-Vivien, M.; Sonke, J.; Hedgecock, I.; Bravo, A.; Rosati, G.; Canu, D.; Horvat, M.; Sprovieri, F.; Pirrone, N.; Heimbürger-Boavida, L. Mediterranean Mercury Assessment 2022: An Updated Budget, Health Consequences, and Research Perspectives. *Environ. Sci. Technol.* **2022**, *56* (7), 3840−3862.
(32) Lu, R.; Colomer-Vidal, P.; Muñoz-Arnanz, J.; García-Barcelona, S.; Zheng, X.; Mai, B.; González-Solís, J.; Jiménez, B. A 20-Year Study Reveal Decrease in per- and Polyfluoroalkyl Substances (PFAS) in a Pelagic Seabird from the Western Mediterranean Sea. *Environ. Pollut.* **2024**, *362*, No. 125025.
(33) Ramos, R.; González-Solís, J.; Forero, M. G.; Moreno, R.; Gómez-Díaz, E.; Ruiz, X.; Hobson, K. A. The Influence of Breeding Colony and Sex on Mercury, Selenium and Lead Levels and Carbon and Nitrogen Stable Isotope Signatures in Summer and Winter Feathers of Calonectris shearwaters. *Oecologia* **2009**, *159* (2), 345−354.
(34) Albertos, S.; Berenguer, N. I.; Sánchez-Virosta, P.; Gómez-Ramírez, P.; Jiménez, P.; Torres-Chaparro, M. Y.; Valverde, I.; Navas, I.; María-Mojica, P.; García-Fernández, A. J.; Espín, S. Mercury Exposure in Birds Linked to Marine Ecosystems in the Western Mediterranean. *Arch. Environ. Contam. Toxicol.* **2020**, *79* (4), 435−453.
(35) Malmberg, J.; White, L.; Vandewoude, S. Bioaccumulation of Pathogen Exposure in Top Predators. *Trends in ecology & evolution* **2021**, *36*, 411.
(36) Xavier, J.; Magalhães, M.; Mendonça, A.; Antunes, M.; Carvalho, N.; Machete, M.; Santos, R.; Paiva, V.; Hamer, K. Changes in Diet of Cory's shearwaters Calonectris diomedea Breeding in the Azores. *Mar. Ornithol.* **2011**, *39*, 129−134.
(37) Thabet, I.; Bourgeois, K.; Le Loc'h, F.; Abdennadher, A.; Munaron, J.-M.; Gharsalli, M.; Romdhane, M. S.; Lasram, F. B. R. Trophic Ecology of Scopoli's shearwaters during Breeding in the Zembra Archipelago (Northern Tunisia). *Marine Biology* **2019**, *166* (5), 61.
(38) Michel, L.; Cianchetti-Benedetti, M.; Catoni, C.; Dell'Omo, G. How shearwaters Prey. New Insights in Foraging Behaviour and Marine Foraging Associations Using Bird-Borne Video Cameras. *Marine Biology* **2022**, *169* (1), 7.
(39) Post, D. M. Using Stable Isotopes to Estimate Trophic Position: Models, Methods and Assumptions. *Ecology* **2002**, *83*, 703−718.
(40) Stier, A.; Romestaing, C.; Schull, Q.; Lefol, E.; Robin, J.-P.; Roussel, D.; Bize, P. How to Measure Mitochondrial Function in Birds Using Red Blood Cells: A Case Study in the King Penguin and

Perspectives in Ecology and Evolution. *Methods in Ecology and Evolution* **2017**, *8* (10), 1172−1182.
(41) Tagliavia, M.; Catania, V.; Dell'Omo, G.; Massa, B. High-Performance PCR for Alleles Discrimination of Chromo-Helicase-DNA Binding Protein (CHD1) Gene in Bird Sexing. *Biology* **2023**, *12* (2), 300.
(42) Zammit, R.; Borg, J. Notes on the Breeding Biology of the Cory's shearwater in the Maltese Islands. *Il-Merill* **1986**, *24*, 1−9.
(43) Müller, M. S.; Massa, B.; Phillips, R. A.; Dell'Omo, G. Seabirds Mated for Life Migrate Separately to the Same Places: Behavioural Coordination or Shared Proximate Causes? *Animal Behaviour* **2015**, *102*, 267−276.
(44) Sait, S. T. L.; Rinø, S. F.; Gonzalez, S. V.; Pastukhov, M. V.; Poletaeva, V. I.; Farkas, J.; Jenssen, B. M.; Ciesielski, T. M.; Asimakopoulos, A. G. Occurrence and Tissue Distribution of 33 Legacy and Novel Per- and Polyfluoroalkyl Substances (PFASs) in Baikal Seals (Phoca Sibirica). *Sci. Total Environ.* **2023**, *889*, No. 164096.
(45) Korner-Nievergelt, F.; Roth, T.; von Felten, S.; Guélat, J.; Almasi, B.; Korner-Nievergelt, P. *Bayesian Data Analysis in Ecology Using Linear Models with R, BUGS, and Stan*, 1st ed.; Academic Press: 2015.
(46) Gelman, A.; Hill, J. *Data Analysis Using Regresion and Multilevel/Hierarchical Models*; Cambridge University Press: Cambridge, 2007.
(47) Nakagawa, S.; Schielzeth, H. Repeatability for Gaussian and Non-Gaussian Data: A Practical Guide for Biologists. *Biological Reviews.* **2010**, *85* (4), 935−956.
(48) R Core Team. *R: A Language and Environment for Statistical Computing*; R Foundation for Statistical Computing: Vienna, Austria, 2020.
(49) Bates, D.; Maechler, M.; Bolker, B.; Walker, S. Fitting Linear Mixed-Effects Models Using Lme4. *Journal of Statistical Software* **2015**, *67* (1), 1−48.
(50) Wickham, H. *Ggplot2: Elegant Graphics for Data Analysis*; Springer-Verlag: New York, 2016.
(51) Martinez-Finley, E. J.; Aschner, M. Recent Advances in Mercury Research. *Current Environmental Health Reports* **2014**, *1* (2), 163−171.
(52) Soldatini, C.; Sebastiano, M.; Albores-Barajas, Y. V.; Abdelgawad, H.; Bustamante, P.; Costantini, D. Mercury Exposure in Relation to Foraging Ecology and Its Impact on the Oxidative Status of an Endangered Seabird. *Science of The Total Environment* **2020**, *724*, No. 138131.
(53) Carravieri, A.; Bustamante, P.; Tartu, S.; Meillère, A.; Labadie, P.; Budzinski, H.; Peluhet, L.; Barbraud, C.; Weimerskirch, H.; Chastel, O.; Cherel, Y. Wandering Albatrosses Document Latitudinal Variations in the Transfer of Persistent Organic Pollutants and Mercury to Southern Ocean Predators. *Environ. Sci. Technol.* **2014**, *48* (24), 14746−14755.
(54) Lavoie, R. A.; Jardine, T. D.; Chumchal, M. M.; Kidd, K. A.; Campbell, L. M. Biomagnification of Mercury in Aquatic Food Webs: A Worldwide Meta-Analysis. *Environ. Sci. Technol.* **2013**, *47* (23), 13385−13394.
(55) Austad, M.; Michel, L.; Masello, J. F.; Cecere, J. G.; De Pascalis, F.; Bustamante, P.; Dell'Omo, G.; Griep, S.; Quillfeldt, P. Diet of Two Mediterranean shearwaters Revealed by DNA Metabarcoding. *Marine Biology* **2025**, *172* (7), 104.
(56) Cianchetti-Benedetti, M.; dell'Omo, G.; Russo, T.; Catoni, C.; Quillfeldt, P. Interactions between Commercial Fishing Vessels and a Pelagic Seabird in the Southern Mediterranean Sea. *BMC Ecol.* **2018**, *18*, 54.
(57) Casagrande, S.; Stier, A.; Monaghan, P.; Loveland, J. L.; Boner, W.; Lupi, S.; Trevisi, R.; Hau, M. Increased Glucocorticoid Concentrations in Early Life Cause Mitochondrial Inefficiency and Short Telomeres. *Journal of Experimental Biology* **2020**, *223* (15), jeb222513.
(58) Stier, A.; Bize, P.; Roussel, D.; Schull, Q.; Massemin, S.; Criscuolo, F. Mitochondrial Uncoupling as a Regulator of Life-History Trajectories in Birds: An Experimental Study in the Zebra Finch. *Journal of Experimental Biology* **2014**, *217* (19), 3579−3589.
(59) Grundlingh, J.; Dargan, P. I.; El-Zanfaly, M.; Wood, D. M. 2,4-Dinitrophenol (DNP): A Weight Loss Agent with Significant Acute Toxicity and Risk of Death. *Journal of Medical Toxicology* **2011**, *7* (3), 205−212.
(60) Granadeiro, J. P.; Nunes, M.; Silva, M. C.; Furness, R. W. Flexible Foraging Strategy of Cory's shearwater, Calonectris diomedea, during the Chick-Rearing Period. *Animal Behaviour* **1998**, *56* (5), 1169−1176.
(61) Casagrande, S.; Dell'Omo, G. Linking Warmer Nest Temperatures to Reduced Body Size in Seabird Nestlings: Possible Mitochondrial bioenergetic and Proteomic Mechanisms. *J. Exp. Biol.* **2025**, *228*, No. jeb.249880.
(62) Burton, G.; Alley, R.; Rasmussen, G.; Orton, P.; Cox, V.; Jones, P.; Graff, D. Mercury and Behavior in Wild Mouse Populations. *Environmental Research* **1977**, *14* (1), 30−34.
(63) Grunst, A. S.; Grunst, M. L.; Grémillet, D.; Kato, A.; Bustamante, P.; Albert, C.; Brisson-Curadeau, É.; Clairbaux, M.; Cruz-Flores, M.; Gentès, S.; Perret, S.; Ste-Marie, E.; Wojczulanis-Jakubas, K.; Fort, J. Mercury Contamination Challenges the Behavioral Response of a Keystone Species to Arctic Climate Change. *Environ. Sci. Technol.* **2023**, *57*, 2054.
(64) Ma, T.; Jiang, Y.; Chen, P.; Xiao, F.; Zhang, J.; Ma, Y.; Chen, T. PFOS and PFOSA Induce Oxidative Stress-Mediated Cardiac Defects in Zebrafish via PPARγ and AHR Pathways, Respectively. *Sci. Total Environ.* **2024**, *951*, No. 175716.
(65) Guo, C.; Zhao, Z.; Zhao, K.; Huang, J.-J.; Ding, L.; Huang, X.; Meng, L.; Li, L.; Wei, H.; Zhang, S. Perfluorooctanoic Acid Inhibits the Maturation Rate of Mouse Oocytes Cultured in Vitro by Triggering Mitochondrial and DNA Damage. *Birth Defects Research* **2021**, *113*, 1074−1083.
(66) Xu, H.; Mao, X.; Zhang, S.; Ren, J.; Jiang, S.; Cai, L.; Miao, X.; Tao, Y.; Peng, C.; Lv, M.; Li, Y. Perfluorooctanoic Acid Triggers Premature Ovarian Insufficiency by Impairing NAD+ Synthesis and Mitochondrial Function in Adult Zebrafish. *Toxicol. Sci.* **2024**, *201* (1), 118−128.
(67) Ask, A. V.; Jenssen, B. M.; Tartu, S.; Angelier, F.; Chastel, O.; Gabrielsen, G. W. Per- and Polyfluoroalkyl Substances Are Positively Associated with Thyroid Hormones in an Arctic Seabird. *Environ. Toxicol. Chem.* **2020**, *40* (3), 820−831.
(68) Agusa, T.; Matsumoto, T.; Ikemoto, T.; Anan, Y.; Kubota, R.; Yasunaga, G.; Kunito, T.; Tanabe, S.; Ogi, H.; Shibata, Y. Body Distribution of Trace Elements in Black-Tailed Gulls from Rishiri Island, Japan: Age-Dependent Accumulation and Transfer to Feathers and Eggs. *Environ. Toxicol. Chem.* **2005**, *24* (9), 2107−2120.
(69) Robinson, S.; Lajeunesse, M.; Forbes, M. Sex Differences in Mercury Contamination of Birds: Testing Multiple Hypotheses with Meta-Analysis. *Environ. Sci. Technol.* **2012**, *46* (13), 7094−7101.
(70) Bustamante, P.; Carravieri, A.; Goutte, A.; Barbraud, C.; Delord, K.; Chastel, O.; Weimerskirch, H.; Cherel, Y. High Feather Mercury Concentrations in the Wandering Albatross Are Related to Sex, Breeding Status and Trophic Ecology with No Demographic Consequences. *Environ. Res.* **2016**, *144* (Pt A), 1−10.
(71) Carravieri, A.; Vincze, O.; Bustamante, P.; Ackerman, J.; Adams, E.; Angelier, F.; Chastel, O.; Cherel, Y.; Gilg, O.; Golubova, E.; Kitaysky, A.; Luff, K.; Seewagen, C.; Strøm, H.; Will, A.; Yannic, G.; Giraudeau, M.; Fort, J. Quantitative Meta-analysis Reveals No Association between Mercury Contamination and Body Condition in Birds. *Biol. Rev.* **2022**, *97*, 1253.
(72) Grémillet, D.; Pichegru, L.; Kuntz, G.; Woakes, A. G.; Wilkinson, S.; Crawford, R. J. M.; Ryan, P. G. A Junk-Food Hypothesis for Gannets Feeding on Fishery Waste. *Proceedings of the Royal Society B: Biological Sciences* **2008**, *275* (1639), 1149−1156.
(73) Le Bot, T.; Lescroël, A.; Fort, J.; Péron, C.; Gimenez, O.; Provost, P.; Grémillet, D. Fishery Discards Do Not Compensate Natural Prey Shortage in Northern Gannets from the English Channel. *Biological Conservation* **2019**, *236*, 375−384.
(74) Xia, W.; Wan, Y.; Li, Y.; Zeng, H.; Lv, Z.; Li, G.; Wei, Z.; Xu, S. PFOS Prenatal Exposure Induce Mitochondrial Injury and Gene Expression Change in Hearts of Weaned SD Rats. *Toxicology* **2011**, *282* (1−2), 23−29.
(75) Zarei, M.; Shirazi, S.; Aghvami, M.; Pourahmad, J. Perfluorooctanesulfonate (PFOS) Induces Apoptosis Signaling and Proteolysis

in Human Lymphocytes through ROS Mediated Mitochondrial Dysfunction and Lysosomal Membrane Labialization. *Iran. J. Pharm. Res* **2018**, *17* (3), 995−1007.
(76) Martínez-Quezada, R.; González-Castañeda, G.; Bahena, I.; Domínguez, A.; Domínguez-López, P.; Casas, E.; Betancourt, M.; Casillas, F.; Rodríguez, J.; Alvarez, L.; Mateos, R.; Altamirano, M.; Bonilla, E. Effect of Perfluorohexane Sulfonate on Pig Oocyte Maturation, Gap-Junctional Intercellular Communication, Mitochondrial Membrane Potential and DNA Damage in Cumulus Cells in Vitro. *Toxicol. In Vitro* **2021**, *70*, No. 105011.
(77) Zhang, Y.; Shu, M.; Shan, S.; Liu, H.; Zhang, Y.; Song, C.; Xu, Q.; Fan, Y.; Lu, C. Perfluorohexane Sulfonic Acid Disrupts the Immune Microenvironment for Spermatogenesis by Damaging the Structure of the Blood-Testis Barrier in Mice. *Advanced Science* **2025**.
(78) Jiao, X.; Liu, N.; Xu, Y.; Qiao, H. Perfluorononanoic Acid Impedes Mouse Oocyte Maturation by Inducing Mitochondrial Dysfunction and Oxidative Stress. *Reproductive Toxicology* **2021**, *104*, 58−67.
(79) Zhang, P.; Qi, C.; Ma, Z.; Wang, Y.; Zhang, L.; Hou, X. Perfluorooctanoic Acid Exposure in Vivo Perturbs Mitochondrial Metabolic during Oocyte Maturation. *Environmental Toxicology* **2022**, *37* (12), 2965−2976.

https://doi.org/10.1021/envhealth.5c00297
Environ. Health 2026, 4, 782−799